Journal Pre-proof

Design, synthesis and biological evaluation of novel *N*-sulfonylamidine-based derivatives as c-Met inhibitors via Cu-catalyzed three-component reaction

Xiang Nan, Jing Zhang, Hui-Jing Li, Rui Wu, Sen-Biao Fang, Zhi-Zhou Zhang, Yan-Chao Wu

PII: S0223-5234(20)30441-4

DOI: https://doi.org/10.1016/j.ejmech.2020.112470

Reference: EJMECH 112470

To appear in: *European Journal of Medicinal Chemistry*

Received Date: 20 April 2020

Revised Date: 9 May 2020

Accepted Date: 13 May 2020

Please cite this article as: X. Nan, J. Zhang, H.-J. Li, R. Wu, S.-B. Fang, Z.-Z. Zhang, Y.-C. Wu, Design, synthesis and biological evaluation of novel *N*-sulfonylamidine-based derivatives as c-Met inhibitors via Cu-catalyzed three-component reaction, *European Journal of Medicinal Chemistry* (2020), doi: https://doi.org/10.1016/j.ejmech.2020.112470.

Graphical Abstract

Design, synthesis and biological evaluation of novel *N*-sulfonylamidine-based derivatives as c-Met inhibitors via Cu-catalyzed three-component reaction

Xiang Nan, Jing Zhang, Hui-Jing Li, Rui Wu, Sen-Biao Fang, Zhi-Zhou Zhang, Yan-Chao Wu

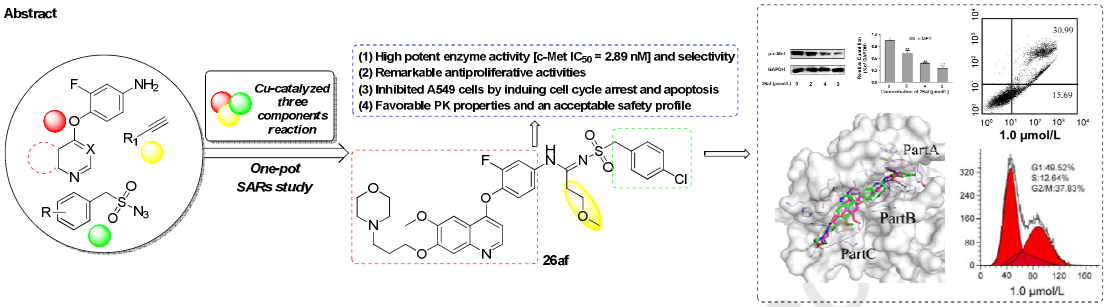

Design, synthesis and biological evaluation of novel *N*-sulfonylamidine-based derivatives as c-Met inhibitors via Cu-catalyzed three-component reaction

Xiang Nan [a], Jing Zhang [b], Hui-Jing Li [a, d, *], Rui Wu [b, *], Sen-Biao Fang [c, *], Zhi-Zhou Zhang [a, d], Yan-Chao Wu [a, d, *]

[a] *School of Marine Science and Technology, Harbin Institute of Technology, Weihai 264209, PR China*

[b] *Department of Pharmacy, the 3201 Affiliated Hospital of Xi'an Jiaotong University, Hanzhong 723000, PR China*

[c] *School of Computer Science and Engineering, Central South University, Changsha 410082, PR China*

[d] *Weihai Institute of Marine Biomedical Industrial Technology, Wendeng District, Weihai 264400, PR China*

Corresponding authors

*Hui-Jing Li: lihuijing@iccas.ac.cn; *Rui Wu: yjk_3201@163.com; *Sen-Biao Fang: fangsb@csu.edu.cn; *Yan-Chao Wu: ycwu@iccas.ac.cn

Abstract

In our continuing efforts to develop novel c-Met inhibitors as potential anticancer candidates, a series of new *N*-sulfonylamidine derivatives were designed, synthesized via Cu-catalyzed multicomponent reaction (MCR) as the key step, and evaluated for their in vitro biological activities against c-Met kinase and four cancer cell lines (A549, HT-29, MKN-45 and MDA-MB-231). Most of the target compounds showed moderate to significant potency at both the enzyme-based and cell-based assay and possessed selectivity for A549 and HT-29 cancer cell lines. The preliminary SAR studies demonstrated that compound **26af** (c-Met IC_{50} = 2.89 nM) was the most promising compound compared with the positive foretinib, which exhibited the remarkable antiproliferative activities, with IC_{50} values ranging from 0.28 to 0.72 μM. Mechanistic studies of **26af** showed the anticancer activity was closely related to the blocking phosphorylation of c-Met, leading to cell cycle arresting at G2/M phase and apoptosis of A549 cells by a concentration-dependent manner. The promising compound **26af** was further identified as a relatively selective inhibitor of c-Met kinase, which also possessed an acceptable safety profile and favorable pharmacokinetic properties in BALB/c mouse. The favorable drug-likeness of **26af** suggested that *N*-sulfonylamidines may be used as a promising scaffold for antitumor drug development. Additionally, the docking study and molecular dynamics simulations of **26af** revealed a common mode of interaction with the binding site of c-Met. These positive results indicated that compound **26af** is a potential anti-cancer candidate for clinical trials, and deserves further development as a selective c-Met inhibitor.

Keywords: *N*-Sulfonylamidine; c-Met inhibitors; Cu-catalyzed three-component reaction; biological evaluation; docking study.

1. Introduction

Mesenchymal-epithelial transition factor (c-Met), also termed as hepatocyte growth factor receptor (HGFR), is a structurally distinct member of heterodimeric transmemeric receptor tyrosine kinase composed of an extracellular α chain and a membrane spanning β chain that are connected by a disulfide bond [1,2]. Phosphorylated c-Met further triggers the activation of downstream signaling pathways such as the Ras/MAPK, c-Src and PI3K/Akt pathways that contributes to the regulation of many physiological processes including cell proliferation, survival, motility, migration, morphogenic differentiation and angiogenesis [3–7]. Aberrant c-Met signaling is implicated in the development and progression in a variety of human solid cancers such as thyroid cancer, lung cancer, gastric cancer, colorectal cancer, pancreatic cancer, prostate cancers, renal cancer, *etc* [8-12]. More importantly, convincing evidences disclosed that both overexpression of c-Met and MET amplification have been correlated with advanced disease stage and poor prognosis [13-15]. Furthermore, crosstalk between c-Met and other receptor tyrosine kinases promotes aggressive tumor behavior and resistance to conventional cancer therapy [16,17]. Therefore, inhibition of the abnormal activation of c-Met/HGF signaling pathway represents one of the most promising therapeutic targets in the discovery of anticancer drugs.

Up to now, many strategies have applied to regulate the abnormal activation of c-Met/HGF signaling pathway and small molecule c-Met kinase inhibitors as one of the most promising approaches has been attracted more and more attention [18-24]. The advantage of small molecule inhibitors via the intracellular kinase domain is that they can effectively block both ligand-dependent and independent activation of c-Met [25-31]. Although the development of small-molecule c-Met tyrosine kinase inhibitors (TKIs) started much later than other strategies, significant progress has been made recently with a considerable number of compounds entering clinical trials or being approved as anticancer drugs (**Fig. 1**). The reported small-molecule inhibitors can be roughly divided into two types according to their structures and binding modes with the kinase catalytic domain of c-Met, namely **type I** and **type II** [32-34]. As reported recently, **type II** inhibitors may be more effective than **type I** inhibitors against the mutations near the active site of c-Met because **type II** inhibitors are assumed to be able to walk away from the gatekeeper and bind beyond the entrance of the c-Met active site [35-39]. Various **type II** c-Met inhibitors have been developed to narrow the gap between bioactive compounds and promising anticancer candidates, leading to some **type II** c-Met inhibitors entering clinical trials [40-43]. However, a poor selectivity profile may make the related **type II** Met inhibitors display a certain degree of toxicity in various organs, or lead to suboptimal dosing for the c-Met inhibition in clinical applications [44,45]. Accordingly, discovery of novel **type II** c-Met inhibitors with improved selectivity profiles, particularly to VEGFR-2, and minimal side effects becomes a high priority [46].

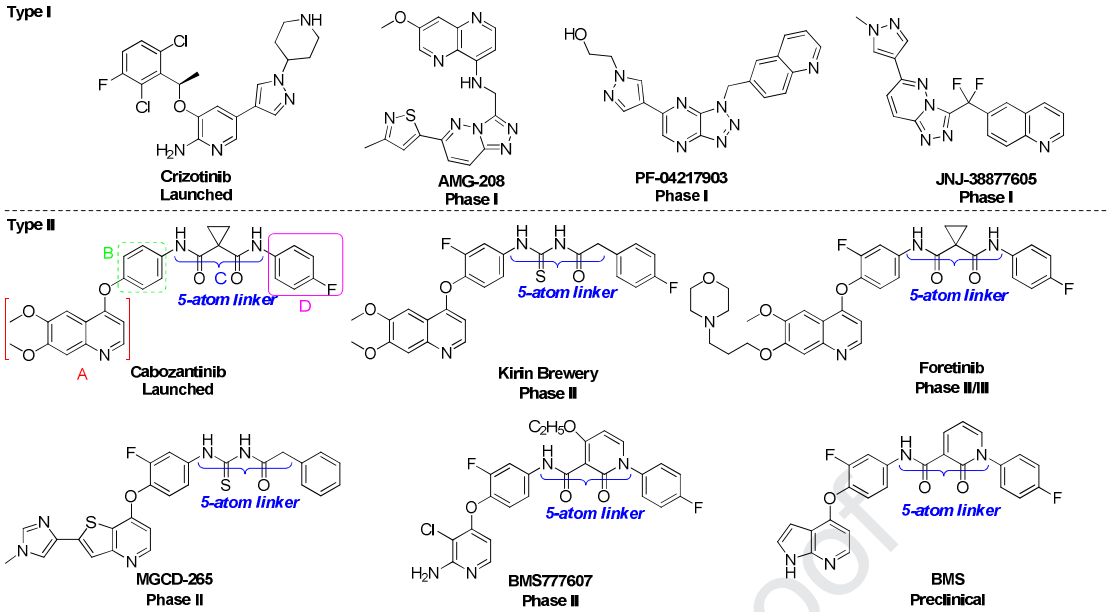

Fig. 1. The representative c-Met kinase inhibitors of different types.

As shown in **Fig. 1**, the structures of **type II** c-Met inhibitors can be disconnected into four units (block A–D) according to their structures and interaction characteristics with protein molecular. Usually, the modification of moiety A and moiety B is constrained since the binding modes of c-Met kinase with **type II** inhibitors. The modification of moiety C, including linear and cyclic fragments between moieties A and B, is the most successful strategy to develop new c-Met inhibitors, which is known as '**5 atoms regulation/hydrogen-bond donors or acceptors**' [47-50]. These structural characteristics indicated that exploring a suitable linker might be a feasible way to discover novel **type II** c-Met inhibitors. Although many efforts have been paid to the construction of the 5-atom linker (**Fig. 2**), one-pot synthesis of the 5-atom linker is still a significant challenge. Multicomponent reactions (MCRs) deemed to satisfy this criterion in view of their ability to generate structurally diverse molecules in a simple one-pot reaction [51,52]. It is worth to note that the marriage of MCRs and combinatorial synthesis has innovated medicinal chemistry by boosting diversification of organic molecules to discover new drug candidates. Amidines [53-55] and sulfonates [56,57] have attracted continuous attention due to their fundamental roles in many selective drugs with low toxicity, sulfonylamidine (**Fig. 2**) could be a potential linker candidate for c-Met inhibitors. To our delight, the sulfonylamidine scaffold also conformed to the characteristics of the '**5 atoms regulation**' and contained both **hydrogen-bond donor and acceptor**. In this context, we hope that by using sulfonylamidine as the 5-atom linker could facilitate the discovery of highly selective c-Met inhibitors. Accordingly, we reported for the first time the one-pot synthesis of the sulfonylamidine linker via Cu-catalyzed modified Click chemistry [58-61], which provided a rapid approach towards the synthesis of new-designed c-Met inhibitors. Meanwhile, various substituents were introduced into the moiety A, moiety D as well as the moiety C (5-atom linker) to investigate the effects on activity. All target compounds were evaluated for their c-Met kinase activity and antiproliferative activities against four cancer cell lines, including H460, HT-29, MKN-45 and MDA-MB-231. Moreover, the cell apoptosis and

cycle arrest, western blotting, acute toxicity, selectivity index, kinase selectivity and pharmacokinetic profiles and docking study of the representative compound **26af** were further explored. Inspiringly, **26af** showed remarkable antiproliferative effects, high selectivity to c-Met *vs* VEGFR-2, favorable pharmacokinetic properties and an acceptable safety profile, which suggested **26af** is a potential anti-cancer candidate for clinical trials, and deserves further development as a selective c-Met inhibitor.

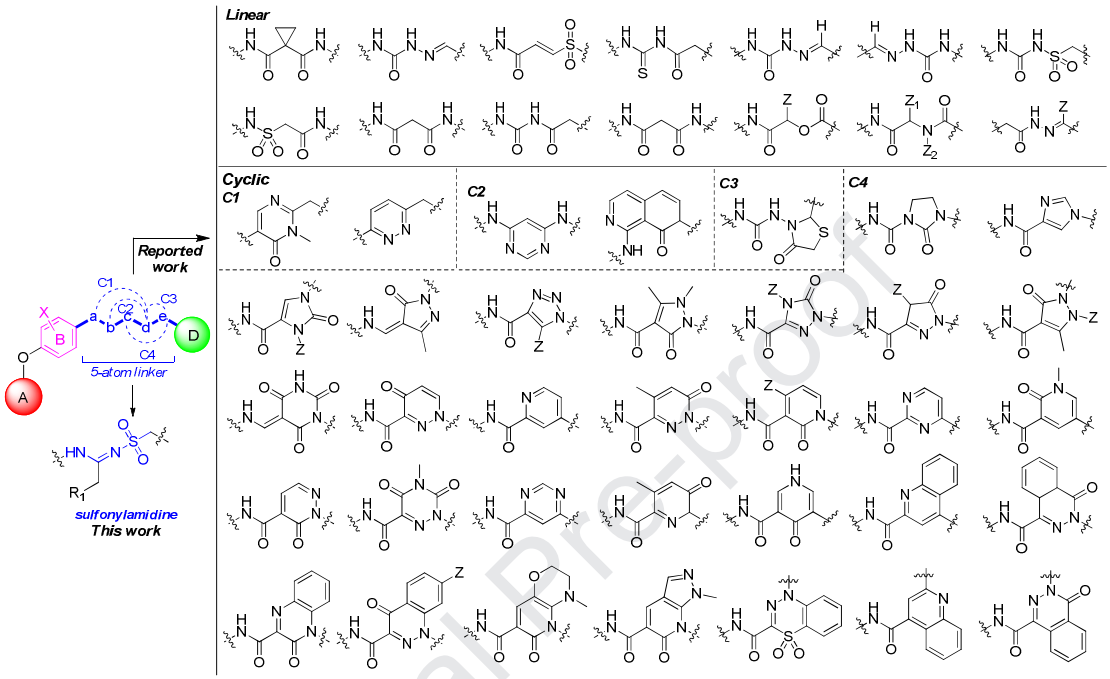

Fig. 2. Various moiety C structures with linear or cyclic 5-atom linkers.

2. Results and discussion

2.1. Chemistry

*2.1.1. Synthesis of 3-fluoro-4-(thieno[3,2-b]pyridin-7-yloxy)aniline (**5**) and 3-fluoro-4-(thieno[3,2-d]pyrimidin-4-yloxy)aniline (**9**)*

As shown in **Scheme 1**, 3-fluoro-4-(thieno[3,2-b]pyridin-7-yloxy)aniline **5** was synthesized from commercially available 3-amino-2-thiophenecarboxylic acid methyl ester, which underwent saponification reaction followed by decarboxylation reaction under basic conditions to afford 3-aminothiophene **1** with good overall yield [62]. Condensation of **1** with Mander's reagent and subsequent intramolecular cyclization in hot diphenyl ether provided 4*H*-thieno[3,2-b]pyridin-7-one **3** in 65% overall yield [63]. 7-Chloro-thieno[3,2-b]pyridine **4** was obtained in 83% yield by treating **3** on exposure of phosphorus oxychloride. Etherification of **4** with 4-amino-2-fluorophenol generated amide **5** in 68% yield, and 20% of **4** was recovered**.** The intermediate **9** was also synthesized starting from 3-amino-2-thiophenecarboxylic acid methyl ester as illustrated in **Scheme 1**. This commercially available material underwent a sequence of formylation, cyclization, and chlorination to afford **8** in 47% overall yield [64]. Coupling of 4-chloro-thieno[3,2-d]pyrimidine **8** with 4-amino-2-fluorophenol in the presence of NaH to yield the intermediate **9**

in 76% yield [65].

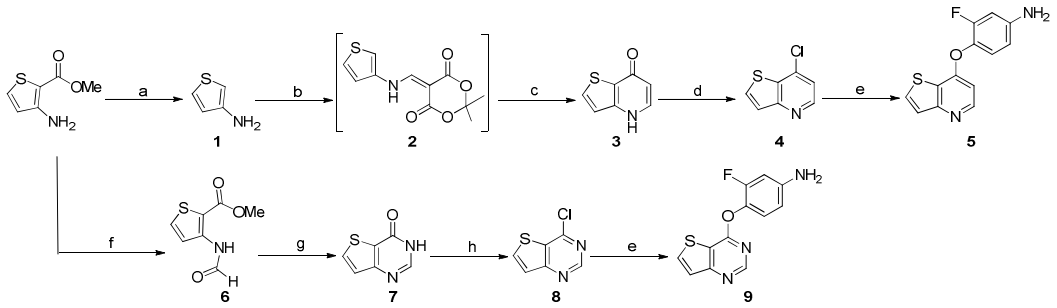

Scheme 1. Reagents and conditions: (a) i) 2 M NaOH, reflux, 30 min; ii) oxalic acid, 1-propanol, 38 °C, 45 min; (b) triethyl orthoformate, 2,2-dimethyl-1,3-dioxane-4,6-dione, 85 °C, overnight; (c) Ph_2O, 240 °C, 30 min; (d) $POCl_3$, DMF (cat.), 0 °C → reflux, 2 h; (e) 4-amino-2-fluorophenol, NaH, DMSO, 0 °C → 60 °C, overnight; (f) HCOOH, Ac_2O, 0 °C → r.t., 12 h; (g) ammonium formate, formamide, 150 °C, 8 h; (h) oxalyl chloride, DMF (cat.), CH_2Cl_2, 0 °C → reflux, 3 h.

*2.1.2. Synthesis of 4-((6,7-dimethoxyquinazolin-4-yl)oxy)-3-fluoroaniline (**14**)*

The synthesis of intermediate **14** was depicted in **Scheme 2**. Regioselective nitration of 3,4-dimethoxybenzoic acid followed hydrogenation with H_2 in the presence of Raney nickel afforded 2-amino-4,5-dimethoxybenzoic acid **11** in 57% overall yield, which underwent an intramolecular cyclization in formamidine to give quinazolinone **12** with good efficiency [66]. Subsequently, chlorination of quinazolinone **12** using phosphorous oxychloride followed by etherification with 4-amino-2-fluorophenol provided amide **14** in 48% overall yield [65].

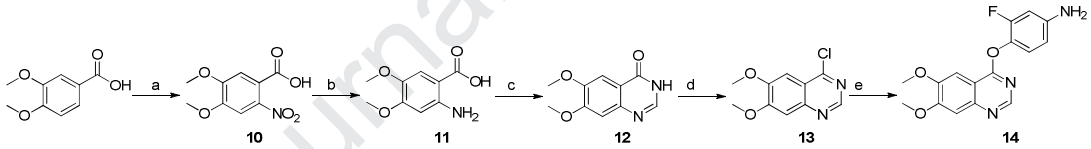

Scheme 2. Reagents and conditions: (a) HNO_3 (20%), 60 °C, 5 h; (b) H_2, Raney nickel, 2-propanol, 40 °C, 5 h; (c) formamide, 150 °C, 8 h; (d) $POCl_3$, 0 °C → reflux, 9 h; (e) 4-amino-2-fluorophenol, NaH, DMSO, 0 °C → 60 °C, overnight.

*2.1.3. Synthesis of 6,7-disubstituted-4-phenoxyquinolines **22a–f***

As shown in **Scheme 3**, the key intermediates of 6,7-disubstituted-4-phenoxyquinolines **22a–f** were synthesized from commercially available 4-hydroxy-3-methoxyacetophenone, which was alkylated with iodomethane, 1-bromobutane or 1-bromo-3-chloropropane under basic reaction conditions to provide **15a–c** in excellent yields. Regioselective nitration and subsequent aminomethylenation with *N*,*N*-dimethylformamide dimethyl acetal (DMF-DMA) to afford intermediates **17a–c**, which underwent an intramolecular cyclization in the presence of iron powder and acetic acid to give **18a–c** with good overall efficiency. Compounds **18a–c** were converted into compounds **19a–c** on exposure of phosphorus oxychloride in high yields. Treatment of **19c** with different secondary amines under basic conditions to generate the intermediates **20a–d**. Compounds **19a–b** and **20a–d** were subjected to a two-step sequence of etherification and hydrogenation for the elegant synthesis of amides **22a–f**.

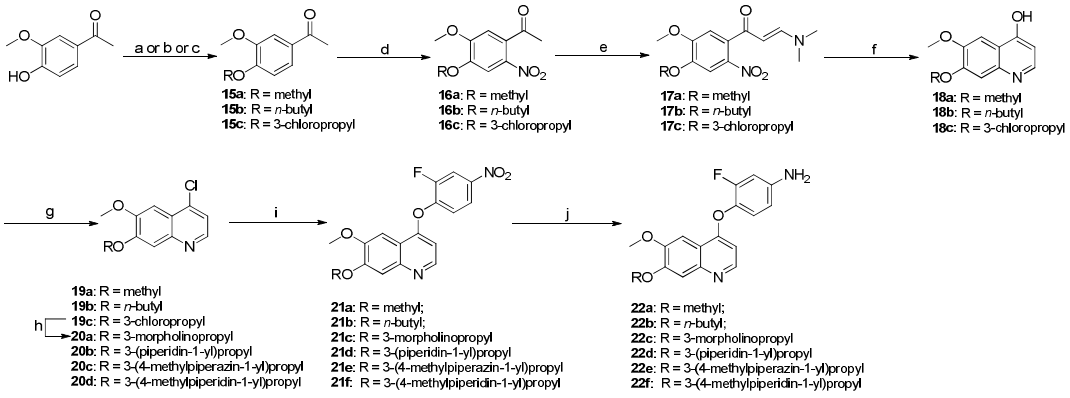

Scheme 3. Reagents and conditions: (a) CH_3I, K_2CO_3, acetone, r.t., 4 h; (b) 1-bromobutane, K_2CO_3, DMF, 80 °C, 10 h; (c) 1-bromo-3-chloropropane, K_2CO_3, DMF, r.t., overnight; (d) concentrated nitric acid (20%), 0 °C, overnight; (e) DMF-DMA, toluene, reflux, 10 h; (f) Fe (powder), AcOH, 80 °C, 2 h; (g) $POCl_3$, DMF (cat.), reflux, 1 h; (h) secondary amines, DMF, NaI, 85 °C, 10 h; (i) 2-fluoro-4-nirophenol, chlorobenzene, 140 °C, 20 h; (j) $SnCl_2.2H_2O$, EtOH, 70 °C, 6 h.

*2.1.4. Synthesis of benzylsulfonyl azides **25a–k***

The condensation of thiourea with different substituted alkyl chlorides **23a–k** followed by chlorosulfonation with *N*-chlorosuccinimide afforded sulfonyl chlorides **24a–k** [67]. Further substitution of **24a–k** with sodium azide provided sulfonyl azides **25a–k** smoothly in moderate overall yields.

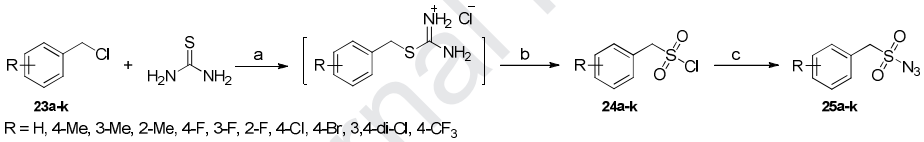

Scheme 4. (a) reflux, 1 h; (b) NCS, 2 M HCl, CH_3CN, 0 °C → r.t., 0.5 h; (c) NaN_3, 0 °C→ r.t., 2 h.

2.1.5. Synthesis of target compounds bearing sulfonylamidine scaffold

A variety of amines **5**, **9**, **14** and **22a–f** were successfully employed as an efficient reacting partner in the Cu-catalyzed three-component reaction in the presence of pyridine catalyst to afford the desired *N*-sulfonylamidine-containing target compounds **26a–am** in moderate to excellent yields [68,69]. The coupling reaction has extremely broad substrate scope with all three components of alkyne, sulfonyl azide and amine. The reaction took place under very mild reaction conditions and displayed excellent functional group compatibility. The reaction possibly proceeds through a ketenimine intermediate, which is generated in situ from the Cu-triazole cycloadduct followed by Dimorph rearrangement via α-diazoimine species readily react with an amine along with release of N_2 gas. Altogether, the Cu-catalyzed three-component coupling reaction could be an efficient and convenient method to combine several active moieties into one molecule, and could be convenient to implement structural modification via alternation of diverse starting materials. All newly synthesized target compounds were purified by column chromatography and their structures were characterized by NMR, MS and elemental analysis.

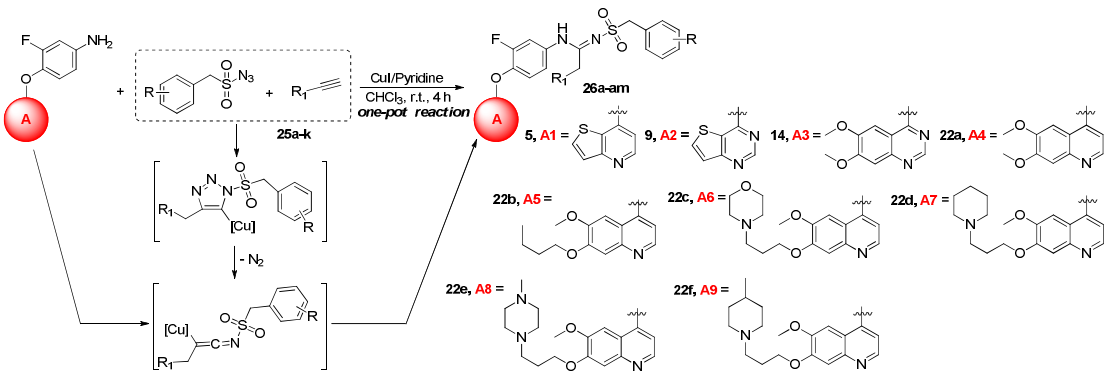

Scheme 5. General synthetic route of target compounds **26a**–**am**.

2.2. Biological evaluation

2.2.1. In vitro enzymatic assays and structure-activity relationships

The c-Met enzymatic assays of all newly synthesized target compounds were evaluated using homogeneous time-resolved fluorescence (HTRF) assay. Foretinib was used as a positive control, and the results expressed as the half-maximal inhibitory concentration (IC_{50}) values were presented in **Table 1**, as mean values of experiments performed in triplicate.

As illustrated in **Table 1**, these novel derivatives bearing *N*-sulfonylamidine moiety were found to be active against c-Met kinase with IC_{50} values ranging from 2.89 to 76.55 nM; three of them (**26af**, IC_{50}= 2.89 nM; **26ah**, IC_{50}= 4.02 nM; **26aj**, IC_{50}= 3.83 nM) showed comparable potency with foretinib (IC_{50}= 2.15 nM), indicating that the introduction of the new moiety *N*-sulfonylamidine as 'five-atom linker' maintained the potent c-Met kinase inhibitory efficacy. The initial SARs study of moiety A was performed. Compounds **26a** (IC_{50} =37.43 nM, R = H, R_1 = *n*-butyl) and **26b** (IC_{50} = 28.62 nM, R = 4-F, R_1 = *n*-butyl) bearing the block thieno[3,2-b]pyridine-7-yl **A1** only displayed moderate c-Met kinase inhibitory activity compared with the positive foretinib. The replacement of the thieno[3,2-b]pyridine **A1** with thieno[3,2-d]pyrimidine **A2** (**26c**, IC_{50} = 60.25 nM, R = H, R_1 = *n*-butyl; **26d**, IC_{50} = 42.48 nM, R = 4-F, R_1 = *n*-butyl) and 6,7-dimethoxyquinazoline **A3** (**26e**, IC_{50} = 74.58 nM, R = H, R_1 = *n*-butyl; **26f**, IC_{50} = 50.87 nM, R = 4-F, R_1 = *n*-butyl) all resulted in a significant loss of potency. Inspiringly, compounds **26g**–**h** (**26g**, IC_{50} = 25.74 nM, R = H, R_1 = *n*-butyl; **26h**, IC_{50} = 20.12 nM; R = 4-F, R_1 = *n*-butyl) bearing the block 6,7-dimethoxyquinoline **A4** displayed greater potency than compounds **26a**–**f**, suggesting that the quinoline pharmacophore is more suitable for vander Waals interactions with the backbone of c-Met kinase. Accordingly, quinoline derivatives were further studied in the following work.

Considering the vital role of 5-atom linker on activity, comprehensive quinoline analogs with diverse R_1 substituents, including phenyl, methoxymethyl, hydrogen atom, 1-cyclohexenyl, 3-pyridyl and 3-thienyl were investigated to further discover the structure-activity relationships. The SARs based on IC_{50} values indicated that the R_1 group played an important role for the c-Met kinase inhibitory efficacy. The introduction of phenyl (**26i**, IC_{50} = 76.55 nM, R = H, R_1 = Phenyl) led to 2.9-fold decrease compared with **26g** (IC_{50} = 25.74 nM, R = H, R_1 = *n*-butyl). Simultaneously, five-membered heterocyclic groups were also

explored, such as 3-pyridyl **26q** (IC_{50} =60.58 nM, R = H, R_1 = 3-pyridyl) and 3-thienyl **26s** (IC_{50} = 55.58 nM, R = H, R_1 = 3-thienyl), which led to 2.4- and 2.2-fold loss activity in against c-Met kinase compared with **26g**, indicating that the electron-rich five membered ring made an adverse effect on c-Met inhibitory potency. Moreover, the replacement *n*-butyl (**26g**, IC_{50} = 25.74 nM, R = H) with 1-cyclohexenyl **26o** (IC_{50} = 50.54 nM, R = H, R_1 = 1-cyclohexenyl) resulted in 1.9-fold loss activity. However, with the introduction of H atom on R_1, compound **26m** (IC_{50} = 20.36 nM, R = H, R_1 = H, increased 1.3-fold) displayed a slight increase on c-Met inhibitory efficacy in comparison with **26g**. To our delight, introduction of methoxymethyl **26k** (IC_{50} = 15.64 nM, R = H, R_1 = methoxymethyl) showed a significant increase on c-Met inhibitory activity. The above results suggested that electronic effect and steric hindrance of R_1 group were sensitive to the c-Met kinase inhibitory activities. Further studies about the effect of R_1 group are in progress in our laboratory and will be reported upon in the future.

With the suitable R_1 group (methoxymethyl) in hand, the influence of substituents on the phenyl ring R was further studied. The SARs based on IC_{50} values also revealed that the R group also played an important role for the c-Met kinase inhibitory efficacy due to its essential interactions with the hydrophobic pocket of c-Met. In comparison with **26k** (IC_{50} = 15.64 nM, R = H) bearing no substituent on phenyl ring, the incorporation of mono-donating groups (mono-EDGs) showed negative tendency in potency, such as **26u** (IC_{50}= 18.72 nM, R = 2-CH_3), **26v** (IC_{50} = 22.45 nM, R = 3-CH_3) and **26w** (IC_{50} = 27.86 nM, R = 4-CH_3). In view of these results, the utilization of EDGs was not further pursed. Inspiringly, introduction of mono-electron-withdrawing groups (mono-EWGs, such as F and Cl) on the phenyl ring showed positive influences on activity. It was worth to note that incorporation of the mono-EWGs at 4-position of the phenyl (**26l**, IC_{50} = 9.12 nM, R = 4-F, increased 1.7-fold) showed a higher preference than that of mono-EWGs at 3-position (**26y**, IC_{50} = 11.36 nM, R = 3-F, increased 1.4-fold) and 2-position of the phenyl (**26x**, IC_{50} = 13.28 nM, R = 2-F, increased 1.2-fold). However, the introduction of double electron-withdrawing groups (**26ab**, IC_{50} = 8.38 nM, R = 3,4-di-Cl) showed a slight decrease on c-Met inhibitory efficacy in comparison with mono-electron-withdrawing derivative (**26z**, IC_{50} = 5.35 nM, R = 4-Cl), which suggested a mono-substituted phenyl ring is more desirable than a disubstituted phenyl ring. The introduction of strong EWGs to phenyl ring derivative **26ac** (IC_{50} = 46.32 nM, R = 4-CF_3, decreased 2.9-fold) resulted in a significantly decrease in activities compared with **26k**, suggesting that the phenyl probably need a properly electron density. The hindrance effect of the bulky substituents likely damped the potency because of the more steric analog **26aa** (IC_{50} = 24.65 nM, R = 4-Br, decreased 1.6-fold) showed obvious decreased activity compared with **26k**, indicating that the hydrophobic pocket of c-Met was fairly sensitive to the size of substituents.

Based on the understanding of the cocrystal structural between c-Met and foretinib, the quinoline portion (moiety A) on the left side not only forms hydrogen bonds with the Pro1158 and Met1160 residues and also maintains vander Waals interactions with the c-Met backbone. In addition, this quinoline system is directed toward a solvent-exposed area, which provides an opportunity for the introduction of polar and hydrophilic groups. Encouraged by these results, analogues contained polar groups

on 7-position of quinoline were prepared for SAR exploration. The replacement the methoxy (**26z**, IC_{50} = 5.35 nM, **A4**, R = 4-Cl, R_1 = methoxymethyl) at the 7-position of quinoline with *n*-butoxy (**26ad**, IC_{50} =12.12 nM, **A5**, R = 4-Cl, R_1 = methoxymethyl) led to a 2.3-fold decrease in c-Met inhibitory activity, which revealed the length of carbon tether was significant to activity. According to the previous research, a three-carbon tether between these amines and the quinoline has been determined to be the optimal length for improving the potency. Thus, different amines at the end of this tether were investigated, and all of them improved the inhibitory potency of c-Met compared with **26z** and **26ab**, which can be explained by the vander Waals interaction between the carbon tether and the c-Met backbone. Based on pharmacological data in **Table 1**, it was found that the introduction of water-soluble group at 7-position of quinoline nucleus had a marked influence on c-Met inhibitory efficacy in the preferential order of morpholinyl > *N*-methyl piperazinyl > piperidinyl > 4-methyl piperidinyl.

The pharmacological data above indicated that the favorable moiety A (quinoline pharmacophore), and the appropriate electronic density and steric hindrance on the 5-atom linker are the main reasons for the inhibitory activity of c-Met kinase. Moreover, the pharmacological data demonstrated that the hydrophobic pocket of c-Met kinase can accommodate the mono-EWGs of the phenyl ring (moiety D), especially the Cl atom at *para*-position of phenyl rings. Additionally, the introduction of different hydrophilic groups at 7-position of quinoline nucleus made a positive influence on c-Met inhibitory efficacy.

Table 1. In vitro c-Met kinase activities of target compounds **26a-am**.

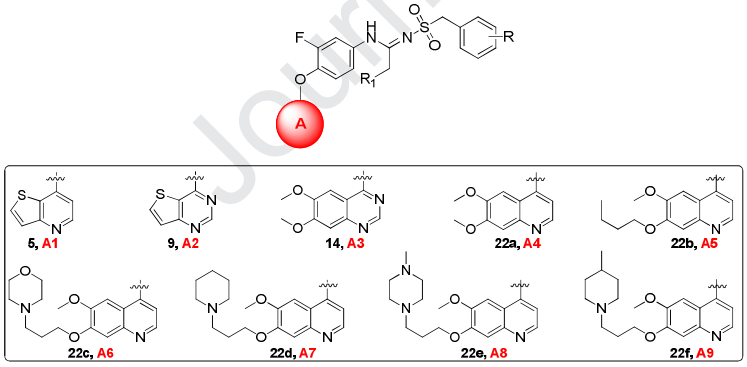

Compd.	A	R_1	R	c-Met IC_{50} (nM)
26a	**A1**	*n*-Butyl	H	37.43 ± 2.56
26b	**A1**	*n*-Butyl	4-F	28.62 ± 2.74
26c	**A2**	*n*-Butyl	H	60.25 ± 4.36
26d	**A2**	*n*-Butyl	4-F	42.48 ± 3.25
26e	**A3**	*n*-Butyl	H	74.58 ± 4.93
26f	**A3**	*n*-Butyl	4-F	50.87 ± 3.45
26g	**A4**	*n*-Butyl	H	25.74 ± 1.98
26h	**A4**	*n*-Butyl	4-F	20.12 ± 1.64
26i	**A4**	Phenyl	H	76.55 ± 5.82

26j	**A4**	Phenyl	4-F	63.26 ± 4.85
26k	**A4**	Methoxymethyl	H	15.64 ± 1.64
26l	**A4**	Methoxymethyl	4-F	9.12 ± 1.26
26m	**A4**	H	H	20.36 ± 2.12
26n	**A4**	H	4-F	16.55 ± 1.84
26o	**A4**	1-Cyclohexenyl	H	50.54 ± 4.66
26p	**A4**	1-Cyclohexenyl	4-F	44.37 ± 3.35
26q	**A4**	3-Pyridyl	H	60.58 ± 4.68
26r	**A4**	3-Pyridyl	4-F	52.72 ± 6.29
26s	**A4**	3-Thienyl	H	55.58 ± 4.47
26t	**A4**	3-Thienyl	4-F	44.25 ± 3.46
26u	**A4**	Methoxymethyl	2-Methyl	18.72 ± 1.54
26v	**A4**	Methoxymethyl	3-Methyl	22.45 ± 2.78
26w	**A4**	Methoxymethyl	4-Methyl	27.86 ± 3.23
26x	**A4**	Methoxymethyl	2-F	13.28 ± 1.76
26y	**A4**	Methoxymethyl	3-F	11.36 ± 0.98
26z	**A4**	Methoxymethyl	4-Cl	5.35 ± 0.63
26aa	**A4**	Methoxymethyl	4-Br	24.65 ± 1.86
26ab	**A4**	Methoxymethyl	3,4-di-Cl	8.38 ± 0.85
26ac	**A4**	Methoxymethyl	4-CF_3	46.32 ± 3.24
26ad	**A5**	Methoxymethyl	4-Cl	12.12 ± 0.95
26ae	**A5**	Methoxymethyl	3,4-di-Cl	16.53 ± 1.69
26af	**A6**	Methoxymethyl	4-Cl	2.89 ± 0.35
26ag	**A6**	Methoxymethyl	3,4-di-Cl	6.26 ± 0.84
26ah	**A7**	Methoxymethyl	4-Cl	4.02 ± 0.51
26ai	**A7**	Methoxymethyl	3,4-di-Cl	8.14 ± 0.83
26aj	**A8**	Methoxymethyl	4-Cl	3.83 ± 0.46
26ak	**A8**	Methoxymethyl	3,4-di-Cl	7.18 ± 0.68
26al	**A9**	Methoxymethyl	4-Cl	5.12 ± 0.65
26am	**A9**	Methoxymethyl	3,4-di-Cl	8.22 ± 0.84
Foretinib				2.15 ± 0.18

2.2.2. In vitro antiproliferative assays of target compounds against four human tumor cell lines

The MTT assay was used to evaluate the cytotoxicity of target compounds to four human tumor cell lines, including three c-Met-addicted cancer cell lines A549 (human lung carcinoma), HT-29 (human colon adenocarcinoma), MKN-45 (human gastric cancer) and a c-Met less-sensitive MDA-MB-231 (triple-negative human breast cancer), taking foretinib as positive control. The results were expressed as half-maximal inhibitory concentration (IC_{50}) values and listed in **Table 2**, as mean values of independent experiments performed in triplicate.

As shown in **Table 2**, most of the target compounds showed moderate to excellent cytotoxic activities to the four tumor cell lines tested in vitro, with IC_{50} values ranging from 0.28 to 32.49 μM. The activity of four target compounds to certain cancer lines was similar or higher than that of foretinib, indicating that the introduction of *N*-sulfonylamidines as the 5-atom linker

maintained significant cytotoxicity. Higher potency was observed that quinoline nucleus as the moiety **A** in comparison with other pharmacophores such as thieno[3,2-b]pyridine **A1**, thieno[3,2-d]pyrimidine **A2** and 6,7-dimethoxyquinazoline **A3**. What's more, most of the target compounds displayed good antiproliferative potency against A549, while the antiproliferative potency against the other three cell lines was relatively poor, indicating that this series of target compounds may possess selectivity for A549 cell. To our delight, the most promising compound **26af** exhibited remarkable cytotoxicity against A549, HT-29 and MDA-MB-231 with IC_{50} values of 0.28 ± 0.04, 0.32 ± 0.03, 0.72 ± 0.06 μM, respectively, which were 1.2–1.5 folds more active than foretinib. The study on structure-activity relationships (SARs) revealed that these analogs showed similar properties as summarized in the c-Met kinase level mentioned above: (I) quinoline nucleus as the moiety **A** generally exhibited higher potency than other pharmacophores such as thieno[3,2-b]pyridine **A1**, thieno[3,2-d]pyrimidine **A2** and quinazoline **A3**; (II) the target compounds showed excellent selectivity toward A549 cell; (III) R_1 were substituted with methoxymethyl afforded favorable cytotoxicity against four human tumor cell lines; (IV) the EWGs (such as F and Cl) on the moiety D benefited to the potency, and the potency of *para*-substituted phenyl ring (moiety D) was higher than that of *ortho*- and *meta*-substituted phenyl rings; (V) bulky electron-withdrawing groups on the phenyl ring (such as Br and CF_3) led to an obvious decrease in cytotoxicity; (VI) different cyclic tertiary amino groups at the 7-position of quinoline were advantageous for the potent cytotoxicity.

Table 2. Cytotoxic activities for target compounds **26a-am** against A549, HT-29, MKN-45 and MDA-MB-231 cell lines in vitro.

Compd.	IC_{50} (μmol/L) ± SD			
	A549	HT-29	MKN-45	MDA-MB-231
26a	8.68 ± 0.95	9.63 ± 0.86	11.46 ± 1.32	15.28 ± 0.97
26b	6.23 ± 0.76	7.06 ± 1.14	9.17 ± 1.28	14.55 ± 1.75
26c	17.28 ± 2.03	18.64 ± 1.54	21.85 ± 1.12	25.55 ± 3.34
26d	10.34 ± 1.33	11.15 ± 0.75	12.46 ± 1.57	16.82 ± 2.65
26e	27.12 ± 1.84	30.52 ± 2.43	ND	ND
26f	18.63 ± 2.12	22.14 ± 2.68	23.36 ± 1.58	31.76 ± 3.46
26g	7.55 ± 0.82	8.26 ± 0.69	9.28 ± 1.08	12.83 ± 1.44
26h	4.60 ± 0.24	5.18 ± 0.52	5.54 ± 0.63	9.04 ± 0.65
26i	28.45 ± 2.65	32.63 ± 2.24	26.33 ± 1.95	ND
26j	20.36 ± 1.82	23.66 ± 2.18	ND	32.49 ± 2.74
26k	3.14 ± 0.42	3.52 ± 0.28	4.05 ± 0.36	6.64 ± 0.57
26l	1.42 ± 0.16	1.68 ± 0.22	2.15 ± 0.25	4.24 ± 0.33
26m	5.16 ± 0.52	5.85 ± 0.35	5.99 ± 0.63	9.29 ± 0.63
26n	3.76 ± 0.25	4.12 ± 0.38	4.55 ± 0.42	7.65 ± 0.52
26o	12.15 ± 0.85	14.46 ± 1.44	16.26 ± 1.14	20.45 ± 1.88
26p	9.43 ± 0.94	10.32 ± 1.45	15.24 ± 1.26	19.65 ± 1.69
26q	18.12 ± 1.35	20.56 ± 1.85	22.86 ± 1.75	28.28 ± 3.16
26r	13.16 ± 0.74	15.45 ± 1.66	18.63 ± 1.45	22.30 ± 2.54
26s	14.26 ± 0.74	16.46 ± 0.85	ND	23.83 ± 3.15
26t	10.06 ± 1.22	11.24 ± 0.96	11.86 ± 1.34	19.52 ± 1.45

26u	4.15 ± 0.36	4.85 ± 0.61	5.16 ± 0.64	8.19 ± 0.91
26v	7.54 ± 0.56	8.02 ± 0.75	9.15 ± 1.16	13.06 ± 1.52
26w	8.02 ± 0.68	8.74 ± 0.94	9.75 ± 1.22	13.66 ± 1.56
26x	2.85 ± 0.35	3.16 ± 0.39	3.26 ± 0.43	5.67 ± 0.63
26y	2.14 ± 0.18	2.47 ± 0.41	3.52. ± 0.45	5.34 ± 0.63
26z	0.62 ± 0.09	0.91 ± 0.07	1.05 ± 0.13	2.32 ± 0.27
26aa	7.14 ± 0.65	8.03 ± 0.92	11.28 ± 1.46	12.12 ± 1.38
26ab	0.71 ± 0.08	0.88 ± 0.12	1.16 ± 0.15	3.32 ± 0.27
26ac	11.35 ± 0.86	13.24 ± 1.12	15.26 ± 1.46	20.37 ± 2.04
26ad	2.56 ± 0.32	2.85 ± 0.28	3.05 ± 0.61	5.46 ± 0.63
26ae	3.53 ± 0.48	4.05 ± 0.51	4.36 ± 0.72	7.19 ± 0.64
26af	**0.28 ± 0.04**	**0.32 ± 0.03**	0.48 ± 0.06	**0.72 ± 0.06**
26ag	0.47 ± 0.08	0.59 ± 0.07	0.72 ± 0.05	1.04 ± 0.12
26ah	**0.35 ± 0.05**	**0.41 ± 0.06**	0.65 ± 0.06	1.12 ± 0.23
26ai	0.67 ± 0.07	0.78 ± 0.05	0.88 ± 0.09	**0.93 ± 0.13**
26aj	**0.32 ± 0.03**	**0.36 ± 0.04**	0.61 ± 0.07	1.24 ± 0.15
26ak	0.61 ± 0.09	0.74 ± 0.06	0.82 ± 0.11	1.35 ± 0.16
26al	**0.38 ± 0.05**	0.55 ± 0.04	0.76 ± 0.08	1.56 ± 0.14
26am	0.72 ± 0.12	0.88 ± 0.09	1.15 ± 0.15	1.98 ± 0.18
Foretinib	0.41 ± 0.05	0.46 ± 0.03	0.064 ± 0.007	0.95 ± 0.09

Bold values show the IC_{50} values of the prepared compounds lower than the values of the positive control foretinib. ND: Not determined.

[a] Used as a positive control.

2.2.3. cell apoptosis and cycle arrest

In view of A549 cell line displayed higher sensitivity than the other three tested cancer cell lines to **26af** in the preliminary cytotoxicity profile, A549 cells were used in our mechanistic study. To investigate the specific mechanisms of antiproliferative activity associated with **26af** on human tumor cells, the effect of **26af** on A-549 cell apoptosis and cells cycle analysis was confirmed indirectly using Flow Cytometer by double staining with FITC-annexin V and propidium iodide. Initially, we investigated the effect of **26af** on apoptosis induction. As shown in **Fig. 3**, the flow cytometric analysis showed significant increase in the percentage of Annexin-FITC/PI-positive apoptotic cells after A549 cells were treated with **26af** with a series of concentrations (0.25, 0.5, and 1.0 μM). Specifically, compared with the control group, compound **26af** (1.0 μM) could significantly induce the late apoptotic (30.99%) and early apoptotic (15.69%), the similar trend was observed in other concentrations (0.25, 0.5 μM). The results indicated that compound **26af** can induce apoptosis in a concentration-dependent manner in the early and late stages of apoptosis. Moreover, the percentage of Annexin-FITC/PI-positive apoptotic cells of **26af** was higher than (annexin V positive cell population: **26af** versus foretinib, early apoptosis: 15.69% versus 11.25%; late apoptosis: 30.99% versus 22.90%) that of foretinib when treated with the same concentration (1.0 μM), which could be concluded that compound **26af** can induce apoptosis of A549 more efficient than foretinib. Subsequently, we examined the effect of **26af** on cell cycle distribution and induction of apoptosis in different phases in A549 cells. As shown in **Fig. 4**, after the cells were treated

with vehicle or various concentrations of **26af** (0.25, 0.5, and 1.0 μM), DNA content of the control group displayed a typical histogram in exponentially growing cells. The increasing concentration of **26af** caused the percentage of A549 cells in G2/M phase was significantly increased by a concentration dependent manner, similar with the effect of foretinib on A549 cells. Taken together, these synergistic results demonstrated that **26af** displayed a significant inhibitory effect on the proliferation of A549 cells, which may be achieved by cell cycle arrest at G2/M phase of cell mitosis and subsequently apoptosis induction in cellular.

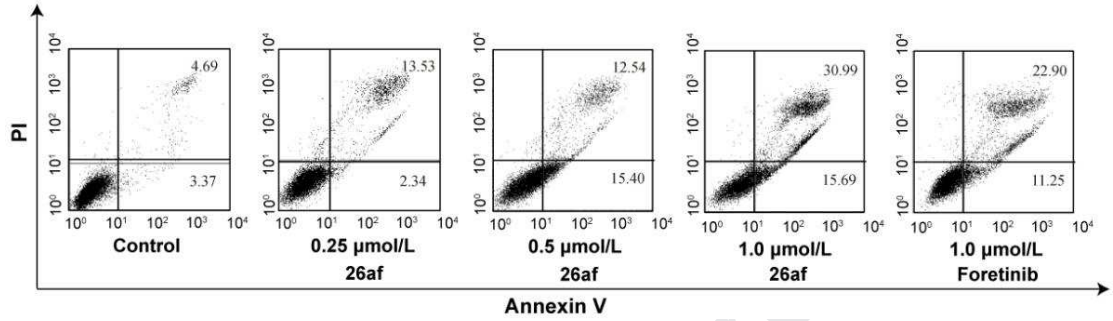

Fig. 3. The effect of **26af** on A549 cells apoptosis by Annexin-FITC/PI double staining.

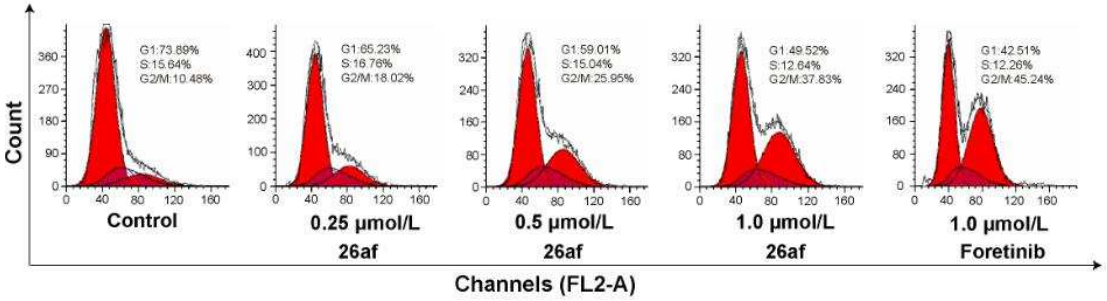

Fig. 4. The effect of **26af** on A549 cells cycle distribution cycle distribution by propidium iodide staining with RNase.

2.2.4. Western blotting analysis of c-Met

Biochemical and cellular cytotoxic data demonstrated that compound **26af** was an excellent c-Met inhibitor. In order to further investigate whether the c-Met kinase inhibition of **26af** in a cell-free system can be recapitulated in vitro, western blotting assay as part of the mechanistic validation was carried out to determine the effect of **26af** on c-Met activation in A549 cells. A549 cells were treated with different concentrations of **26af** for 1 h or DMSO as negative control. Afterwards, the cells were harvested, lysed and subjected to western blotting analysis with the antibodies of phospho-Met (Tyr1234/1235), in which the level of GAPDH served as loading control. As shown in **Fig. 5**, compound **26af** showed excellent inhibition against c-Met phosphorylation in a concentration-dependent manner. These data are consistent with the biochemical and cellular cytotoxic potency (**Table 1, 2**), which suggested that compound **26af** inhibited the activity of c-Met contributes mainly to the suppression of A549 cell proliferation regardless of the mechanistic complexity in c-Met signaling pathways and crosstalk with other receptor tyrosine kinases.

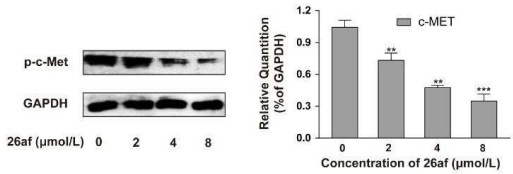

Fig. 5. Effect of compound **26af** on c-Met kinase phosphorylation in A549 cells.

2.2.5. Acute toxicity test

To explore the safety profile of these *N*-sulfonylamidine derivatives, the acute toxicity of **26af** was evaluated in mice. Sixty 8-week-old male BALB/c mice were randomized into six groups (n = 10) to receive 0 (vehicle only), 100, 200, 300, or 400 mg/kg of **26af** intraperitoneal injection on day zero. One group was kept without treatment as a normal control. Animals were observed for 15 days. Treatment with **26af** at 400, 300 mg/kg killed 50%, 30% of the mice, respectively. At the lower dose (0, 100, and 200 mg/kg), all treated animals showed no abnormalities, anaphylactic responses, allergic reactions, significant body weight loss and even animal deaths and were as healthy as the normal control animals throughout the experiment. These results (**Table 3**) suggested that administration of **26af** at or below 200 mg/kg (*i.p.*) may be safe for mice.

Table 3. Acute toxicity profile of compound **26af**.

Does (mg/kg)	Mice (N)	Deaths (N)	Survival on day 15 (%)
400	10	5	50
300	10	3	70
200	10	0	100
100	10	0	100
Vehicle	10	0	100
Normal	10	0	100

2.2.6. Selectivity index

In order to find out whether these *N*-sulfonylamidine derivatives are selective to normal cells, the cytotoxicity of compound **26af** against Human umbilical vein endothelial cells (HUVEC) and human normal colorectal mucosa epithelial cell (FHC) were evaluated. As shown in **Table 4**, the results demonstrated that compound **26af** was found to be more selective to normal cells than to cancer cells in comparison with foretinib. The selectivity index of compound **26af** to HUVEC, FHC cells were 4.2 and 19.1, respectively, which was superior to that of the positive foretinib (selectivity index to HUVEC, 0.9; FHC, 8.3). Based on the results, we could infer that compound **26af** has moderate selectivity towards cancer cells over normal cells.

Table 4. The cytotoxicity of compound **26af** against HUVEC, FHC, and HT-29 cell lines.

Compd.	IC_{50} (μmol/L) ± SD		
	HUVEC	FHC	HT-29
26af	1.35 ± 0.21	6.12 ± 0.56	0.32 ± 0.03
Foretinib	0.42 ± 0.05	3.83 ± 0.42	0.46 ± 0.06

2.2.7. Enzymatic selectivity assays

Considering its remarkable potency against c-Met kinase in vitro and in vivo, compound **26af** was selected to further investigate the kinase selectivity profile. The inhibitory activity of **26af** against a panel of kinases including c-Met family member Ron, highly homologous kinase ALK and other seven tyrosine kinases were assayed using the homogeneous time resolved fluorescence (HTRF) method (**Table 5**). In contrast to its high potency against c-Met (IC_{50} = 2.89 nM), **26af** also exhibited high inhibitory effects against c-Kit (IC_{50} = 4.26 nM) and Flt-3 (IC_{50} = 7.28 nM). Moreover, **26af** demonstrated moderate selectivity against PDGFRα, PDGFRβ, Ron, VEGFR-2 and Flt-4 kinase (133-fold, 196-fold, 143-fold, 233-fold, 124-fold, respectively). Additionally, **26af** exhibited a slight or no tyrosine kinase inhibitory activity against EGFR and ALK (IC_{50} > 10 μM). Compared with foretinib, **26af** significantly increased the selectivity for VEGFR-2, which provide a novel scaffold to investigate the selectivity and reduce VEGFR-2 related side effects. In summary, all the evidences mentioned above suggested that **26af** was a relatively selective inhibitor of c-Met kinase.

Table 5. Kinase selectivity profile of compound **26af** and foretinib.

Enzyme	**Enzyme IC_{50} (nM)**	
	26af	Foretinib
c-kit	4.26	6.52
PDGFRα	384	5.52
PDGFRβ	565	10.63
Ron	412	3.92
VEGFR-2	673	4.26
EGFR	>10,000	3180
Flt-3	7.28	5.24
ALK	>10,000	>5,000
Flt-4	358	4.95
c-Met	2.89	2.15

*2.2.8. Pharmacokinnetic (PK) profile of the selected compound **26af***

With its remarkable in vitro enzyme and cell potencies, the pharmacokinetic properties of oral and intravenous administrated **26af** were further evaluated in BALB/c mouse, and the results were summarized in **Table 6**. After oral administration, compound **26af** (8 mg/kg) presented favorable PK profiles, in briefly, rapid absorption (T_{max}= 2.5 h), high maximum concentration (C_{max} = 1228.4 ng/mL), high plasma exposure ($AUC_{0-\infty}$ = 6.8 μg.h.mL^{-1}), accepted elimination half-life ($T_{1/2}$ = 3.5 h), and well clearance (1.18 L.h^{-1}.kg^{-1}). After intravenous injecting **26af** (2 mg/kg), the maximum concentration was 675.6 ng/mL, plasma exposure was 2.3 μg·h·mL^{-1}, and elimination half-life was 1.8 h. To our delight, compound **26af** had a moderate oral bioavailability (74%) in mouse. Given the promising overall PK profiles and the novelty of *N*-sulfonylamidine moiety, which suggested compound **26af** could be a potential candidate for cancer therapy deserving further study.

Table 6. Pharmacokinetic profiles of compound **26af** in BALB/c mouse.

Route	Does (mg/kg)	$T_{1/2}$ (h)	C_{max} (ng.mL^{-1})	T_{max} (h)	$AUC_{0-\infty}$ (μg.h.mL^{-1})	*CL* (L.h^{-1}.kg^{-1})	*F* (%)
i.v.	2	1.8	675.6	—	2.3	—	
p.o.	8	3.5	1228.4	2.5	6.8	1.18	74

2.3. Molecular docking studies and molecular dynamics (MD) simulations

To further explore the binding modes of target compounds with the active site of c-Met, molecular docking simulation studies were carried out by using Autodock 4.2 package. Based on the in vitro inhibition results, we selected compound **26af**, the best c-Met inhibitor in this study, as ligand example, and the structures of c-Met/VEGFR-2 were selected as the docking model (PDB ID code: 3LQ8, 3U6J, respectively). In blind docking process, the one conformation with the lowest binding energy was used to predict the protein-aptamer binding spots. The binding modes of compound **26af** with c-Met or VEGFR-2 were shown in **Fig. 6A**, **6B**, respectively. As shown in **Fig. 6A**, the nitrogen atom of quinoline, the oxygen atom of sulfonyl group in compound **26af** formed two H-bond interactions with residue Met1160 and Lys1110 of c-Met, respectively. One π-π interaction between the 2-fluorophenyl ring of compound **26af** and Phe1223 has been formed simultaneously. Inspiringly, the nitrogen atom of morpholine formed one H-bond interaction with residue Asn1171. In contrast, the nitrogen atom of quinoline, the nitrogen atom of NH in **26af** only formed two H-bond interactions with VEGFR-2 residue Cys919 and Thr916 as shown in **Fig. 6B**. The differences between the two binding modes (c-Met *vs* VEGFR-2) might be the main reasons that the c-Met selective preferred than VEGFR-2 in terms of compound **26af**. More importantly, the complex structure of **26af**/c-Met (**Fig. 6A**, -20.57 kcal/mol) with lower binding energy from precise docking process compared with **26af**/VEGFR-2 (**Fig. 6B**, -8.53 kcal/mol).

The results obtained from the above docking analysis provoked us to explore the dynamic behavior of c-Met-**26af**/foretinib complexes. A total of 10 ns simulation time was conducted and MDs trajectory was employed for extracting the refined binding model (**Fig. 6C**). The binding interface were mainly located at three regions, part A, part B and part C, one schematic diagram for each region were shown in **Fig. 6D**, **Fig. 6E** and **Fig. 6F**. In part A, the terminal 4-chlorophenyl ring of **26af** fitted into the hydrophobic pocket which was formed hydrophobic amino residues Val1155, Leu1157, Thr1126, Met1131, Ile1130, Phe1134, Phe1200, Leu1195, Val1139 and Leu1140, *etc*. Compared with foretinib, the terminal phenyl ring moiety of **26af** was not fully exposed to the hydrophobic pocket, which made the hydrophobic effects of **26af** seemed to be relatively weaker than that of foretinib. In part B, the oxygen atom of sulfonyl group in compound **26af** formed a H-bond with residue Lys1110. Additionly, a salt-bridge effects was observed between the oxygen atom of sulfonyl group and residue Lys1110 because of Lys belongs to polar amino acid. Moreover, the branch chain of -CH_2-CH_2-O-CH_3 formed hydrophobic interactions with another hydrophobic pocket that consisted of Asp1222, Asn1209, Phe1223, Met1211, Leu1140 and Leu1157, *etc*. The results suggested that the interactions of *N*-sulfonylamidine moiety might be the main reasons that the antiproliferative activities of **26af** was superior to that of foretinib. For part C, the nitrogen atom of quinoline in compound **26af** formed one H-bond with residue Met1160, which

was similar with the complex of foretinib/c-Met. To our surprise, the nitrogen atom of morpholine formed another H-bond interaction with the residue Asn1171. In summary, these results of the docking studies and MD simulations showed that 4-phenoxyquinoline derivatives containing *N*-sulfonylamidine moiety could act synergistically to interact with the binding sites of c-Met, suggesting that the *N*-sulfonylamidine moiety could serve as an excellent platform from which to develop potential antitumor candidates.

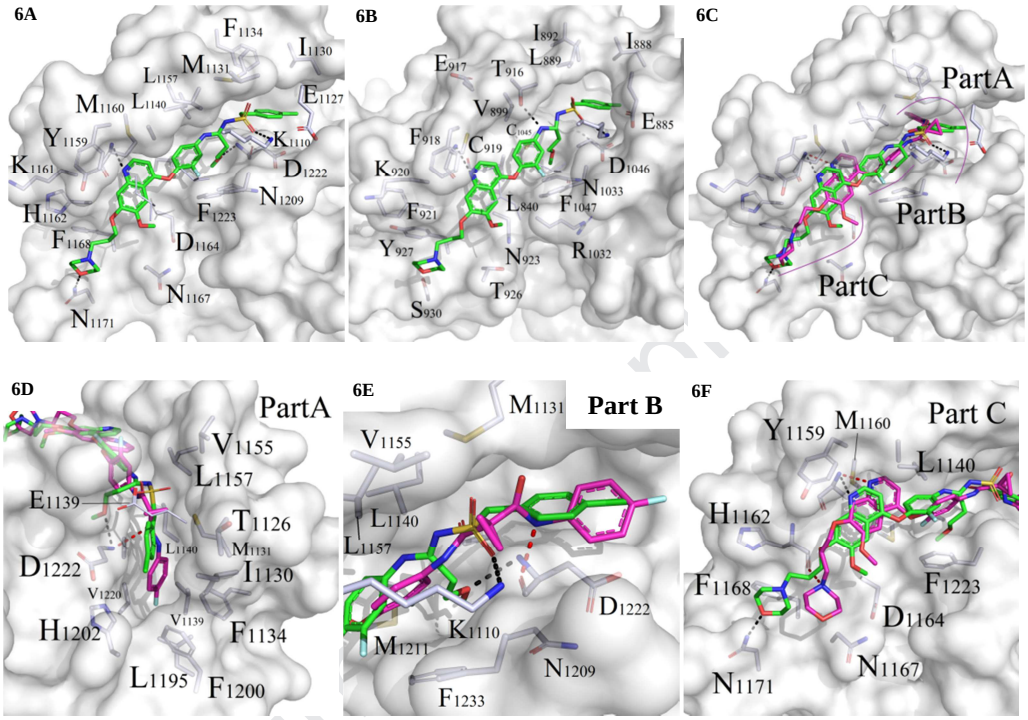

Fig. 6. (A) Binding pose of compound **26af** with the active site of c-Met. Compound **26af** was showed in colored sticks, green: carbon atom, blue: nitrogen atom, pink: oxygen atom, yellow: sulfur atom. (B) Binding pose of compound **26af** with the active site of VEGFR-2. (C) Overlay of **26af** (green color) in the same cavity along with foretinib (pink color) as the reference molecule (A, B and C). (D) The interaction details of part A. (E) The interaction details of part B. (F) The interaction details of part C.

3. Conclusion

In summary, different *N*-sulfonylamidine derivatives as potent c-Met inhibitors were designed, synthesized and evaluated employing a well-planned optimization strategy to investigate the influence of linkers as well as different moieties A and D on the expected antitumor activity. Most of the target compounds demonstrated potent antiproliferative activities in A549, HT-29, MKN-45 and MDA-MB-231 cell lines as well as c-Met kinase, which suggested the introduction of *N*-sulfonylamidineas as the 5-atom linker maintained or even increased the potent activity. The preliminary SAR studies was carried out, and **26af** was identified as the most potent and relatively selective c-Met inhibitor at both the enzyme-based and cell-based assay compared with that of foretinib. The cell cycle and apoptosis results proved that compound **26af** presented a significant inhibitory effect on the proliferation of A549 cells, which may be achieved by periodic blocking and apoptosis induction in the G2/M phase. Furthermore, **26af** inhibited phosphorylation levels of c-Met protein in A549 cells by a dose-dependent manner. In addition, the

safety profiles of **26af** were further studied and no obvious toxicity was observed in acute toxicity tests. Molecular docking of **26af** into ATP binding site of c-Met and VEGFR-2 was performed, and the results suggested that **26af** could bind with the active site of c-Met better than that of VEGFR-2. Meanwhile, the preliminary results in vivo reflected that compound **26af** possessed promising overall PK profiles, and the favorable drug-likeness of **26af** indicated that *N*-sulfonylamidine could be used a novel scaffold for the development of c-Met inhibitors. Collectively, these positive results highlight that c-Met inhibitor **26af** is a potential antitumor candidate, warranting further investigation and development.

4. Experimental

4.1. Chemistry

Common reagents and materials were purchased from commercial sources and were used without further purification unless otherwise noted. Organic solvents were routinely dried and/or distilled prior to use and stored over molecular sieves under argon. Analytical thin layer chromatography (TLC) was performed on precoated silica gel 60 GF254 plates. Flash column chromatography was run on silica gel (200-300 mesh) from Qingdao Ocean Chemicals (Qingdao, Shandong, China). Visualization on TLC was achieved by use of UV light (254 nm) or iodine. ^{1}H and ^{13}C NMR spectra were recorded on Bruker Avance III 400 MHz NMR using tetramethylsilane (TMS) as internal standard. The chemical shifts are expressed in ppm and coupling constants are given in Hz. Data for ^{1}H NMR are recorded as follows: chemical shift (δ, ppm), multiplicity (s = singlet; d = doublet; t = triplet; q = quarter; p = pentet; m = multiplet; br = broad), coupling constant (Hz), integration. Data for ^{13}C NMR are reported in terms of chemical shift (δ, ppm). Mass spectra were recorded on a Bruker Daltonics APEXII49e spectrometer with ESI source as ionization. Melting points were measured by using a Gongyi X-5 microscopy digital melting point apparatus and are uncorrected. Elemental analysis was performed on an Elemental Analyzer vario EL Cube instrument. All yields are unoptimized and generally represent the result of a single experiment.

*4.1.1. General procedure for preparation of 3-fluoro-4-(thieno[3,2-b]pyridin-7-yloxy)aniline (**5**), 3-fluoro-4-(thieno[3,2-d]pyrimidin-4-yloxy)aniline (**9**) and 4-((6,7-dimethoxyquinazolin-4-yl)oxy)-3-fluoroaniline (**14**)*

According to the reported methods as shown in **Scheme 1** and **Scheme 2**, the preparation of intermediates **5**, **9** and **14** were obtained in a multistep process start with commercially available 3-amino-2-thiophenecarboxylic acid methyl ester and 3,4-dimethoxybenzoic acid, respectively. And thus the details of synthesis were not be listed here.

*4.1.1.1. 3-fluoro-4-(thieno[3,2-b]pyridin-7-yloxy)aniline (**5**)*

Yellow solid, m.p.: 112–114 °C. ^{1}H NMR (400 MHz, DMSO-d_6) δ 8.49 (d, J = 5.2 Hz, 1 H), 8.13 (d, J = 5.6 Hz, 1 H), 7.57 (d, J = 5.6 Hz, 1 H), 7.10 (t, J = 9.2 Hz, 1 H), 6.57 (d, J = 5.2 Hz, 1 H), 6.53 (dd, J = 2.4, 13.2 Hz, 1 H), 6.45 (dd, J = 2.0, 8.4 Hz, 1 H), 5.55 (br s, 2 H). ^{13}C NMR (100 MHz, DMSO-d_6) δ 160.1, 158.7, 154.4 (d, J = 242.1 Hz), 149.5, 148.9 (d, J = 10.3 Hz), 132.0,

128.8 (d, *J* = 12.5 Hz), 124.9, 124.1 (d, *J* = 1.6 Hz), 120.5, 110.0 (d, *J* = 2.1 Hz), 102.8, 101.3 (d, *J* = 20.7 Hz). ESI-MS: *m/z* 261.1 $[M+H]^+$.

*4.1.1.2. 3-fluoro-4-(thieno[3,2-d]pyrimidin-4-yloxy)aniline (**9**)*

Brown solid, m.p.: 159–161 °C. ^{1}H NMR (400 MHz, DMSO-d_6) δ 8.70 (s, 1 H), 8.46 (d, *J* = 5.2 Hz, 1 H), 7.66 (d, *J* = 5.6 Hz, 1 H), 7.08 (t, *J* = 9.2 Hz, 1 H), 6.50 (dd, *J* = 2.0, 12.8 Hz, 1 H), 6.42 (dd, *J* = 1.6, 8.4 Hz, 1 H), 5.47 (br s, 2 H). ^{13}C NMR (100 MHz, DMSO-d_6) δ 163.5, 163.1, 154.3 (d, *J* = 241.4 Hz), 154.2, 148.7 (d, *J* = 10.3 Hz), 137.3, 127.9 (d, *J* = 13.1 Hz), 124.2, 116.2, 109.5 (d, *J* = 1.8 Hz), 101.0 (d, *J* = 20.9 Hz). ESI-MS: *m/z* 262.1 $[M+H]^+$.

*4.1.1.3. 4-((6,7-dimethoxyquinazolin-4-yl)oxy)-3-fluoroaniline (**14**)*

Brown solid, m.p.: 225–227 °C. ^{1}H NMR (400 MHz, DMSO-d_6) δ 8.56 (s, 1 H), 7.52 (s, 1 H), 7.40 (s, 1 H), 7.02 (t, *J* = 8.4 Hz, 1 H), 6.52 (dd, *J* = 2.4 Hz, *J* = 12.8 Hz, 1 H), 6.42 (dd, *J* = 2.0 Hz, *J* = 8.4 Hz, 1 H), 5.39 (br s, 2 H), 3.96 (s, 3 H) , 3.94 (s, 3 H). ^{13}C NMR (100 MHz, DMSO-d_6) δ 164.5, 155.7, 154.3 (d, *J* = 241.2 Hz), 152.2, 150.0, 148.7, 148.3 (d, *J* = 10.3 Hz), 128.5 (d, *J* = 13.0 Hz), 124.1, 109.5, 109.2, 106.7, 101.1 (d, *J* = 21.0 Hz), 100.5, 56.1, 55.9. ESI-MS: *m/z* 316.1 $[M+H]^+$.

*4.1.2. General procedure for preparation of 3-fluoro-4-(6,7-disubstituted quinolin-4-yloxy)anilines (**22a-f**)*

The preparation of intermediates **22a**–**f** has been illustrated in detail in our previous work [70] as shown in **Scheme 3**, so the synthesis method would not be listed here.

*4.1.2.1. 4-((6,7-Dimethoxyquinolin-4-yl)oxy)-3-fluoroaniline (**22a**)*

White solid, m.p.: 193–195 °C. ^{1}H NMR (400 MHz, DMSO-d_6) δ 8.45 (d, *J* = 5.6 Hz, 1 H), 7.51 (s, 1 H), 7.38 (s, 1 H), 7.07 (t, *J* = 8.4 Hz, 1 H), 6.56 (dd, *J* = 2.4, 13.2 Hz, 1 H), 6.47 (dd, *J* = 2.0, 8.8 Hz, 1 H), 6.39 (d, *J* = 5.2 Hz, 1 H), 5.50 (s, 2 H), 3.93 (s, 6 H). ^{13}C NMR (100 MHz, DMSO-d_6) δ 160.0, 154.3 (d, *J* = 242.0 Hz), 152.4, 149.1, 148.8, 148.5 (d, *J* = 10.4 Hz), 146.1, 129.2 (d, *J* = 12.5 Hz), 124.0, 114.4, 110.0, 107.7, 101.4, 101.2, 98.9, 55.6. ESI-MS: *m/z* 315.2 $[M+H]^+$.

*4.1.2.2. 4-((7-Butoxy-6-methoxyquinolin-4-yl)oxy)-3-fluoroaniline (**22b**)*

Light yellow solid, m.p.: 196–198 °C. ^{1}H NMR (400 MHz, $CDCl_3$) δ 8.45 (d, *J* = 5.2 Hz, 1 H), 7.57 (s, 1 H), 7.40 (s, 1 H), 7.02 (t, *J* = 8.8 Hz, 1 H), 6.55 (dd, *J* = 2.8, 12.0 Hz, 1 H), 6.50–6.47 (m, 1 H), 6.39 (d, *J* = 5.2 Hz, 1 H), 4.19 (t, *J* = 6.8 Hz, 2 H), 4.03 (s, 3 H), 1.96-1.88 (m, 2 H), 1.58–1.49 (m, 2 H), 0.99 (t, *J* = 7.2 Hz, 3 H). ^{13}C NMR (100 MHz, $CDCl_3$) δ 160.8, 155.0 (d, *J* = 246.8 Hz), 152.3, 149.7, 148.5, 146.5, 145.6 (d, *J* = 9.5 Hz), 132.5 (d, *J* = 12.6 Hz), 124.3, 115.3, 110.0 (d, *J* = 2.9 Hz), 108.3, 103.7 (d, *J* = 21.2 Hz), 101.7, 99.6, 68.6, 56.1, 30.7, 19.2, 13.8. ESI-MS: *m/z* 357.2 $[M+H]^+$.

*4.1.2.3. 3-Fluoro-4-((6-methoxy-7-(3-(morpholin-4-yl)propoxy)quinolin-4-yl)oxy)aniline (**22c**)*

Light yellow solid, m.p.: 217–219 °C. ^{1}H NMR (400 MHz, $CDCl_3$) δ 8.45 (d, *J* = 5.2 Hz, 1 H), 7.56 (s, 1 H), 7.41 (s, 1 H), 7.02 (t, *J* = 8.8 Hz, 1 H), 6.57–6.53 (m, 1 H), 6.49 (dd, *J* = 1.6, 8.4 Hz, 1 H), 6.39 (d, *J* = 5.2 Hz, 1 H), 4.26 (t, *J* = 6.4 Hz, 2 H), 4.02 (s, 3 H), 3.71 (t, *J* = 4.4 Hz, 4 H), 2.57 (t, *J* = 7.2 Hz, 2 H), 2.48–2.44 (m, 4 H), 2.14–2.10 (m, 2 H). ^{13}C NMR (100 MHz,

$CDCl_3$) δ 160.8, 155.1 (d, J = 247.6 Hz), 152.1, 149.7, 148.9, 146.7, 145.7 (d, J = 9.6 Hz), 132.5 (d, J = 12.7 Hz), 124.4, 115.5, 111.0 (d, J = 2.9 Hz), 108.6, 103.7 (d, J = 21.2 Hz), 101.9, 99.7, 67.2, 67.0, 56.2, 55.4, 53.7, 26.0. ESI-MS: m/z 450.2 $[M+Na]^+$.

*4.1.2.4. 3-Fluoro-4-((6-methoxy-7-(3-(piperdine-1-yl)propoxy)quinolin-4-yl)oxy)aniline (**22d**)*

Light yellow solid, m.p.: 194–196 °C. ^{1}H NMR (400 MHz, $CDCl_3$) δ 8.45 (d, J = 5.2 Hz, 1 H), 7.57 (s, 1 H), 7.38 (s, 1 H), 7.02 (t, J = 8.8 Hz, 1 H), 6.56 (dd, J = 2.4, 12.0 Hz, 1 H), 6.50 (d, J = 8.4 Hz, 1 H), 6.40 (d, J = 5.2 Hz, 1 H), 4.24 (t, J = 6.0 Hz, 2 H), 4.01 (s, 3 H), 2.86–2.82 (m, 4 H), 2.40–2.36 (m, 2 H), 1.88–1.85 (m, 4 H), 1.61–1.57 (m, 4 H). ^{13}C NMR (100 MHz, DMSO-d_6) δ 160.6, 154.8 (d, J = 241.1 Hz), 152.3, 149.8, 149.3, 149.0 (d, J = 10.8 Hz), 146.7, 129.7 (d, J = 12.7 Hz), 124.4, 114.9, 110.6, 108.9, 102.0 (d, J = 5.5 Hz), 101.8, 99.6, 67.2, 56.2, 55.6, 54.6, 26.6, 26.1, 24.6. ESI-MS: m/z 426.3 $[M+H]^+$.

*4.1.2.5. 3-Fluoro-4-((6-methoxy-7-(3-(4-methylpiperazine-1-yl)propoxy)quinolin-4-yl)oxy)aniline (**22e**)*

Light yellow solid, m.p.: 202–204 °C. ^{1}H NMR (400 MHz, $CDCl_3$) δ 8.45 (d, J = 5.2 Hz, 1 H), 7.57 (s, 1 H), 7.40 (s, 1 H), 7.02 (t, J = 8.8 Hz, 1 H), 6.58 (dd, J = 2.4, 12.0 Hz, 1 H), 6.54 (dd, J = 2.4, 9.2 Hz, 1 H), 6.41 (d, J = 5.2 Hz, 1 H), 4.26 (t, J = 6.4 Hz, 2 H), 4.03 (s, 3 H), 2.64–2.50 (m, 8 H), 2.16 (s, 3 H), 2.11 (t, J = 10.8 Hz, 2 H), 1.91–1.87 (m, 2 H). ^{13}C NMR (100 MHz, $CDCl_3$) δ 160.7, 155.1 (d, J = 246.5 Hz), 152.2, 149.7, 148.8, 146.7, 145.8 (d, J = 9.5 Hz), 132.4 (d, J = 12.5 Hz), 124.3 (d, J = 1.9 Hz), 115.4, 111.0 (d, J = 2.7 Hz), 108.6, 103.6 (d, J = 21.2 Hz), 101.8, 99.7, 67.3, 56.1, 55.1, 54.9, 53.1, 46.0, 26.3. ESI-MS: m/z 441.3 $[M+H]^+$.

*4.1.2.6. 3-Fluoro-4-((6-methoxy-7-(3-(4-methylpiperdine-1-yl)propoxy)quinolin-4-yl)oxy)aniline (**22f**)*

Light yellow solid, m.p.: 190–192 °C. ^{1}H NMR (400 MHz, $CDCl_3$) δ 8.45 (d, J = 5.2 Hz, 1 H), 7.59 (s, 1 H), 7.40 (s, 1 H), 7.05 (t, J = 8.8 Hz, 1 H), 6.54 (dd, J = 2.4, 12.0 Hz, 1 H), 6.50 (dd, J = 2.8, 8.8 Hz, 1 H), 6.41 (d, J = 5.2 Hz, 1 H), 4.26 (t, J = 6.4 Hz, 2 H), 4.02 (s, 3 H), 2.96 (d, J = 11.6 Hz, 2 H), 2.61–2.57 (m, 2 H), 2.16–2.14 (m, 2 H), 1.96 (t, J = 10.8 Hz, 2 H), 1.65 (d, J = 10.4 Hz, 2 H), 1.32–1.29 (m, 3 H), 0.96 (d, J = 6.0 Hz, 3 H). ^{13}C NMR (100 MHz, $CDCl_3$) δ 160.7, 155.1 (d, J = 246.5 Hz), 152.2, 149.7, 148.8, 146.7, 145.8 (d, J = 9.5 Hz), 132.5 (d, J = 12.7 Hz), 124.4, 115.4, 111.0, 108.7, 103.7 (d, J = 21.1 Hz), 101.8, 99.7, 67.5, 56.1, 55.4, 54.0, 34.2, 30.8, 26.4, 21.9. ESI-MS: m/z 440.2 $[M+H]^+$.

*4.1.3. General procedure for preparation of sulfonyl azides **24a–k***

Various alkyl halides **23a–k** (2.5 mmol) and thiourea (0.19 g, 2.5 mmol) were refluxed together in EtOH (2.5 mL) for 1 h. After removal of EtOH at reduced pressure, the obtained solid was slowly added to a mixture of NCS (1.33 g, 10 mmol), 2 M HCl (0.68 mL) and MeCN (4 mL) over 15 min. Upon completion of the reaction (TLC monitoring), the solvent was removed under vacuum. Then H_2O (5 mL) was added to the residue and stirred for 15 min, the resulting solid was filtered and dried under an infrared lamp to afford the corresponding sulfonyl chlorides **24a-k**. Without further purification, **24a-k** was added in portions to a solution of NaN_3 (195 mg, 3 mmol) in acetone/H_2O (10 mL, acetone/H_2O = 1:1) at 0 °C. After being stirred at room temperaturefor 4 h, the reaction mixture was concentrated in vacuo and H_2O (10 mL) was added to the residue. The aqueous

solution was extracted with $CHCl_3$ (3 × 10 mL). The combined organic layers were washed with brine, dried over Na_2SO_4, filtered and concentrated under reduced pressure to afford sulfonyl azides **25a–k**.

*4.1.3.1. Phenylmethanesulfonyl azide (**25a**)*

White solid, yield: 65%, m.p.: 50–52 °C. ^{1}H NMR (400 MHz, $CDCl_3$) δ 7.48–7.44 (m, 5 H), 4.54 (s, 2 H). ^{13}C NMR (100 MHz, $CDCl_3$) δ 131.0, 129.9, 129.3, 126.7, 61.6. ESI-MS: *m*/*z* 198.0 $[M+H]^+$.

*4.1.3.2. (2-Methylphenyl)methanesulfonyl azide (**25b**)*

White solid, yield: 57%, m.p.: 38–40 °C. ^{1}H NMR (400 MHz, $CDCl_3$) δ 7.42 (d, *J* = 7.6 Hz, 1 H), 7.34 (d, *J* = 6.4 Hz, 1 H), 7.29–7.27 (m, 2 H), 4.61 (s, 2 H), 2.48 (s, 3 H). ^{13}C NMR (100 MHz, $CDCl_3$) δ 138.7, 131.9, 131.3, 130.1, 126.8, 125.2, 59.4, 19.7. ESI-MS: *m*/*z* 212.1 $[M+H]^+$.

*4.1.3.3. (3-Methylphenyl)methanesulfonyl azide (**25c**)*

White solid, yield: 66%, m.p.: 39–41 °C. ^{1}H NMR (400 MHz, $CDCl_3$) δ 7.29–7.27 (m, 1 H), 7.24–7.22 (m, 2 H), 7.20 (s, 1 H), 4.44 (s, 2 H), 2.34 (s, 3 H). ^{13}C NMR (100 MHz, $CDCl_3$) δ 139.1, 131.6, 130.6, 129.1, 128.0, 126.5, 61.9, 21.3. ESI-MS: *m*/*z* 212.1 $[M+H]^+$.

*4.1.3.4. (4-Methylphenyl)methanesulfonyl azide (**25d**)*

White solid, yield: 78%, m.p.: 56–58 °C. ^{1}H NMR (400 MHz, $CDCl_3$) δ 7.34 (d, *J* = 8.0 Hz, 2 H), 7.24 (d, *J* = 7.6 Hz, 2 H), 4.49 (s, 2 H), 2.39 (s, 3 H). ^{13}C NMR (100 MHz, $CDCl_3$) δ 140.1, 130.8, 129.9, 123.6, 61.7, 21.3. ESI-MS: *m*/*z* 212.1 $[M+H]^+$.

*4.1.3.5. (2-Fluorophenyl)methanesulfonyl azide (**25e**)*

White solid, yield: 69%, m.p.: 40–42 °C. ^{1}H NMR (400 MHz, $CDCl_3$) δ 7.51–7.43 (m, 2 H), 7.25–7.16 (m, 2 H), 4.63 (s, 2 H). ^{13}C NMR (100 MHz, $CDCl_3$) δ 161.4 (d, *J* = 249.0 Hz), 132.7 (d, *J* = 2.2 Hz), 132.1 (d, *J* = 8.2 Hz), 125.0 (d, *J* = 3.7 Hz), 116.1 (d, *J* = 21.2 Hz), 114.4 (d, *J* = 14.2 Hz), 54.9. ESI-MS: *m*/*z* 216.0 $[M+H]^+$.

*4.1.3.6. (3-Fluorophenyl)methanesulfonyl azide (**25f**)*

White solid, yield: 74%, m.p.: 48–50 °C. ^{1}H NMR (400 MHz, $CDCl_3$) δ 7.48–7.43 (m, 1 H), 7.27–7.17 (m, 3 H), 4.55 (s, 2 H). ^{13}C NMR (100 MHz, $CDCl_3$) δ 162.8 (d, *J* = 246.7 Hz), 130.9 (d, *J* = 8.3 Hz), 128.8 (d, *J* = 7.8 Hz), 126.8 (d, *J* = 3.0 Hz), 118.0 (d, *J* = 22.3 Hz), 117.1 (d, *J* = 21.0 Hz), 61.3. ESI-MS: *m*/*z* 216.1 $[M+H]^+$.

*4.1.3.7. (4-Fluorophenyl)methanesulfonyl azide (**25g**)*

White solid, yield: 82%, m.p.: 43–45 °C. ^{1}H NMR (400 MHz, $CDCl_3$) δ 7.47–7.44 (m, 2 H), 7.14 (t, *J* = 8.4 Hz, 2 H), 4.51 (s, 2 H). ^{13}C NMR (100 MHz, $CDCl_3$) δ 163.7 (d, *J* = 249.1 Hz), 132.9 (d, *J* = 8.7 Hz), 122.6, 116.5 (d, *J* = 21.8 Hz), 61.0. ESI-MS: *m*/*z* 216.1 $[M+H]^+$.

*4.1.3.8. (4-Chlorophenyl)methanesulfonyl azide (**25h**)*

White solid, yield: 85%, m.p.: 65–67 °C. ^{1}H NMR (400 MHz, $CDCl_3$) δ 7.44–7.39 (m, 4 H), 4.50 (s, 2 H). ^{13}C NMR (100

MHz, $CDCl_3$) δ 136.3, 132.3, 129.6, 125.2, 61.1. ESI-MS: *m*/*z* 232.0 $[M+H]^+$.

*4.1.3.9. (4-Bromophenyl)methanesulfonyl azide (**25i**)*

White solid, yield: 85%, m.p.: 71–73 °C. ^{1}H NMR (400 MHz, $CDCl_3$) δ 7.59 (d, *J* = 8.4 Hz, 2 H), 7.34 (d, *J* = 8.4 Hz, 2 H), 4.48 (s, 2 H). ^{13}C NMR (100 MHz, $CDCl_3$) δ 132.6, 132.5, 125.7, 124.5, 61.2. ESI-MS: *m*/*z* 276.1 $[M+H]^+$.

*4.1.3.10. (3,4-Dichlorophenyl)methanesulfonyl azide (**25j**)*

White solid, yield: 65%, m.p.: 72–74 °C. ^{1}H NMR (400 MHz, $CDCl_3$) δ 7.56 (d, *J* = 2.0 Hz, 1 H), 7.53 (d, *J* = 8.0 Hz, 1 H), 7.31 (dd, *J* = 2.4, 8.4 Hz, 1 H), 4.47 (s, 2 H). ^{13}C NMR (100 MHz, $CDCl_3$) δ 134.7, 133.6, 132.8, 131.3, 130.1, 126.7, 60.5. ESI-MS: *m*/*z* 288.0 $[M+Na]^+$.

*4.1.3.11. (4-Trifluoromethylphenyl)methanesulfonyl azide (**25k**)*

White solid, yield: 48%, m.p.: 81–83 °C. ^{1}H NMR (400 MHz, $CDCl_3$) δ 7.72 (d, *J* = 8.0 Hz, 2 H), 7.61 (d, *J* = 8.0 Hz, 2 H), 4.59 (s, 2 H). ^{13}C NMR (100 MHz, $CDCl_3$) δ 132.1 (q, *J* = 32.8 Hz), 131.5, 130.7, 126.3 (q, *J* = 3.7 Hz), 123.7 (q, *J* = 270.8 Hz), 61.2. ESI-MS: *m*/*z* 266.0 $[M+H]^+$.

*4.1.4. General synthetic procedure for target compounds **26a-am***

To a stirred mixture of CuI (0.042 mmol), sulfonyl azide (0.48 mmol) and alkyne (0.52 mmol) in $CHCl_3$ (10 mL), amine nucleophile (0.4 mmol) was added slowly at room temperature under an N_2 atmosphere. Pyridine (0.52 mmol) was added prior to the addition of nucleophiles. After the reaction was completed, as monitored with TLC, the reaction mixture was diluted by adding $CHCl_3$ (10 mL) and saturated aqueous NH_4Cl solution (20 mL). The mixture was stirred for an additional 30 min and two layers were separated. The aqueous layer was extracted with $CHCl_3$ (3 × 20 mL). The combined organic layers were dried over anhydrous $MgSO_4$, filtered, and concentrated in vacuo. The residue was purified by flash chromatography on silica gel using a mixture of hexane and ethyl acetate as eluent to afford compounds **26a**–**am**.

*4.1.4.1. N'-(Benzylsulfonyl)-N-(3-fluoro-4-(thieno[3,2-b]pyridin-7-yloxy)phenyl)hexanamidine (**26a**)*

White solid, yield: 74%, m.p.: 99–101 °C. ^{1}H NMR (400 MHz, $CDCl_3$) δ 8.53 (s, 1 H), 7.78 (d, *J* = 5.2 Hz, 1 H), 7.58 (d, *J* = 5.2 Hz, 1 H), 7.46–7.33 (m, 5 H), 7.24–7.15 (m, 2 H), 6.68 (s, 1 H), 6.50 (d, *J* = 4.8 Hz, 1 H), 4.35 (s, 2 H), 2.10–1.97 (m, 2 H), 1.74–1.53 (m, 2 H), 1.30–1.21 (m, 4 H), 0.86 (d, *J* = 7.2 Hz, 3 H). ^{13}C NMR (100 MHz, $CDCl_3$) δ 168.0, 160.0, 158.6, 153.9 (d, *J* = 248.5 Hz), 148.8, 137.1 (d, *J* = 11.3 Hz), 136.8 (d, *J* = 9.1 Hz), 131.5, 131.2, 130.8, 129.7, 128.6, 128.5, 124.7, 123.3, 118.2, 111.5 (d, *J* = 22.0 Hz), 103.2, 61.1, 35.6, 31.6, 27.9, 22.2, 13.9. Anal. Calcd. For $C_{26}H_{26}FN_3O_3S_2$: C, 61.04; H, 5.12; N, 8.21. Found: C, 61.05; H, 5.10; N, 8.23. ESI-MS: *m*/*z* 512.2 $[M+H]^+$.

*4.1.4.2. N-(3-Fluoro-4-(thieno[3,2-b]pyridin-7-yloxy)phenyl)-N'-((4-fluorobenzyl)sulfonyl)hexanamidine (**26b**)*

White solid, yield: 78%, m.p.: 92–94 °C. ^{1}H NMR (400 MHz, $CDCl_3$) δ 8.53 (d, *J* =4.8 Hz, 1 H), 7.79 (d, *J* = 5.2 Hz, 1 H), 7.59 (d, *J* = 5.2 Hz, 1 H), 7.42–7.39 (m, 2 H), 7.20–7.02 (m, 4 H), 6.84–6.78 (m, 1 H), 6.51 (d, *J* = 5.2 Hz, 1 H), 4.31 (s, 2 H),

2.04–1.94 (m, 2 H), 1.76–1.56 (m, 2 H), 1.32–1.27 (m, 4 H), 0.86 (t, *J* = 6.8 Hz, 3 H). ^{13}C NMR (100 MHz, $CDCl_3$) δ 168.1, 162.9 (d, *J* = 246.3 Hz), 160.1, 158.4, 153.9 (d, *J* = 247.9 Hz), 148.6, 137.1 (d, *J* = 13.3 Hz), 136.8 (d, *J* = 7.0 Hz), 132.5 (d, *J* = 7.8 Hz), 131.7, 125.7, 124.6, 123.3, 122.4, 118.2, 115.6 (d, *J* = 21.5 Hz), 111.6 (d, *J* = 22.9 Hz), 103.2, 60.2, 35.7, 31.6, 27.9, 22.2, 13.8. Anal. Calcd. For $C_{26}H_{25}F_2N_3O_3S_2$: C, 58.96; H, 4.76; N, 7.93. Found: C, 58.98; H, 4.77; N, 7.95. ESI-MS: *m*/*z* 530.1 $[M+H]^+$.

*4.1.4.3. N'-(Benzylsulfonyl)-N-(3-fluoro-4-(thieno[3,2-d]pyrimidin-4-yloxy)phenyl)hexanamidine (**26c**)*

White solid, yield: 82%, m.p.: 123–125 °C. ^{1}H NMR (400 MHz, $CDCl_3$) δ 8.69 (s, 1 H), 8.02 (d, *J* = 5.2 Hz, 1 H), 7.60 (d, *J* = 5.6 Hz, 1 H), 7.56–7.32 (m, 6 H), 7.18–7.10 (m, 1 H), 6.70–6.64 (m, 1 H), 4.35 (s, 2 H), 1.82–1.53 (m, 4 H), 1.34–1.21 (m, 4 H), 0.88 (t, *J* = 6.8 Hz, 3 H). ^{13}C NMR (100 MHz, $CDCl_3$) δ 167.9, 163.4, 163.1, 154.0, 153.9 (d, *J* = 247.5 Hz), 136.4 (d, *J* = 9.0 Hz), 136.1 (d, *J* = 13.9 Hz), 135.9, 131.2, 130.9, 129.7, 128.6, 128.4, 124.4, 123.7, 118.1, 111.4 (d, *J* = 22.7 Hz), 61.1, 35.6, 31.5, 27.7, 22.2, 13.9. Anal. Calcd. For $C_{25}H_{25}FN_4O_3S_2$: C, 58.58; H, 4.92; N, 10.93. Found: C, 58.60; H, 4.90; N, 10.94. ESI-MS: *m*/*z* 513.2 $[M+H]^+$.

*4.1.4.4. N-(3-Fluoro-4-(thieno[3,2-d]pyrimidin-4-yloxy)phenyl)-N'-((4-fluorobenzyl)sulfonyl)hexanamidine (**26d**)*

White solid, yield: 84%, m.p.: 118–120 °C. ^{1}H NMR (400 MHz, $CDCl_3$) δ 8.67 (s, 1 H), 8.01 (d, *J* = 4.8 Hz, 1 H), 7.56 (d, *J* = 5.2 Hz, 2 H), 7.42–7.33 (m, 2 H), 7.20–7.07 (m, 2 H), 6.99 (t, *J* = 8.0 Hz, 1 H), 6.79–6.74 (m, 1 H), 4.27 (s, 2 H), 1.72–1.53 (m, 2 H), 1.27–1.23 (m, 6 H), 0.83 (t, *J* = 6.4 Hz, 3 H). ^{13}C NMR (100 MHz, $CDCl_3$) δ 168.0, 163.4, 162.9, 162.8 (d, *J* = 245.7 Hz), 153.9, 153.8 (d, *J* = 248.2 Hz),136.4 (d, *J* = 9.4 Hz), 132.2, 136.1, 132.6 (d, *J* = 7.7 Hz), 125.7, 124.3, 123.7, 118.2, 117.4, 115.6 (d, *J* = 21.5 Hz), 111.6 (d, *J* = 22.3 Hz), 60.2, 35.6, 31.5, 27.7, 22.2, 13.9. Anal. Calcd. For $C_{25}H_{24}F_2N_4O_3S_2$: C, 56.59; H, 4.56; N, 10.56. Found: C, 56.61; H, 4.59; N, 10.55. ESI-MS: *m*/*z* 531.1 $[M+H]^+$.

*4.1.4.5. N'-(Benzylsulfonyl)-N-(4-((6,7-dimethoxyquinazolin-4-yl)oxy)-3-fluorophenyl)hexanamidine (**26e**)*

White solid, yield: 68%, m.p.: 132–134 °C. ^{1}H NMR (400 MHz, $CDCl_3$) δ 8.56 (s, 1 H), 7.56–7.30 (m, 8 H), 7.21–7.13 (m, 1 H), 6.69–6.62 (m, 1 H), 4.31 (s, 2 H), 4.04 (s, 3 H), 4.03 (s, 3 H), 2.14–2.11 (m, 2 H), 1.70–1.53 (m, 2 H), 1.27–1.20 (m, 4 H), 0.83 (t, *J* = 6.8 Hz, 3 H). ^{13}C NMR (100 MHz, $CDCl_3$) δ 167.8, 164.6, 156.2, 153.9 (d, *J* = 246.7 Hz), 152.5, 150.5, 149.5, 136.7 (d, *J* = 13.5 Hz), 136.1 (d, *J* = 9.2 Hz), 131.2, 130.9, 129.8, 128.6, 128.4, 123.8, 118.1, 111.5 (d, *J* = 24.0 Hz), 106.7, 100.9, 61.1, 56.5, 56.4, 35.6, 31.6, 27.7, 22.2, 13.9. Anal. Calcd. For $C_{29}H_{31}FN_4O_5S$: C, 61.47; H, 5.51; N, 9.89. Found: C, 61.45; H, 5.54; N, 9.90. ESI-MS: *m*/*z* 589.2 $[M+Na]^+$.

*4.1.4.6. N-(4-((6,7-Dimethoxyquinazolin-4-yl)oxy)-3-fluorophenyl)-N'-((4-fluorobenzyl)sulfonyl)hexanamidine (**26f**)*

White solid, yield: 75%, m.p.: 124–126 °C. ^{1}H NMR (400 MHz, $CDCl_3$) δ 8.56 (s, 1 H), 7.55–7.53 (m, 2 H), 7.42–7.34 (m, 2 H), 7.28 (s, 1 H), 7.20 (t, *J* = 8.0 Hz, 1 H), 7.12–7.05 (m, 1 H), 7.00 (t, *J* = 8.0 Hz, 1 H), 6.79–6.74 (m, 1 H), 4.26 (s, 2 H), 4.04 (s, 3 H), 4.02 (s, 3 H), 2.19–2.14 (m, 2 H), 1.71–1.53 (m, 2 H), 1.26–1.23 (m, 4 H), 0.83 (t, *J* = 6.4 Hz, 3 H). ^{13}C NMR (100 MHz,

$CDCl_3$) δ 167.9, 164.6, 162.9 (d, J = 246.3 Hz), 156.2, 153.9 (d, J = 247.5 Hz), 152.4, 150.5, 149.5, 136.9 (d, J = 12.0 Hz), 135.0 (d, J = 8.5 Hz), 132.6 (d, J = 8.2 Hz), 125.7, 123.9, 118.2, 115.5 (d, J = 21.6 Hz), 111.7 (d, J = 23.4 Hz), 110.1, 106.7, 100.9, 60.2, 56.4, 35.6, 31.5, 27.7, 22.2, 13.9. Anal. Calcd. For $C_{29}H_{30}F_2N_4O_5S$: C, 59.58; H, 5.17; N, 9.58. Found: C, 59.59; H, 5.15; N, 9.61. ESI-MS: m/z 607.2 $[M+Na]^+$.

*4.1.4.7. N'-(Benzylsulfonyl)-N-(4-((6,7-dimethoxyquinolin-4-yl)oxy)-3-fluorophenyl)hexanamidine (**26g**)*

White solid, yield: 76%, m.p.: 141–143 °C. ^{1}H NMR (400 MHz, $CDCl_3$) δ 8.46 (d, J = 5.2 Hz, 1 H), 7.65 (d, J = 11.6 Hz, 1 H), 7.56 (s, 1 H), 7.50–7.41 (m, 3 H), 7.37 (s, 1 H), 7.30–7.29 (m, 2 H), 7.22–7.20 (m, 1 H), 7.12 (t, J = 8.4 Hz, 1 H), 6.36 (d, J = 4.4 Hz, 1 H), 4.33 (s, 2 H), 4.02 (s, 3 H), 3.98 (s, 3 H), 2.78–2.63 (m, 2 H), 1.75–1.72 (m, 2 H), 1.22–1.20 (m, 4 H), 0.80 (t, J = 6.0 Hz, 3 H). ^{13}C NMR (100 MHz, $CDCl_3$) δ 167.9, 160.1, 154.0 (d, J = 246.5 Hz), 153.1, 149.8, 148.5, 146.7, 137.8 (d, J = 12.7 Hz), 136.3 (d, J = 9.5 Hz), 130.8, 129.8, 128.6, 128.4, 123.4, 118.2, 115.6, 111.7 (d, J = 23.3 Hz), 107.4, 102.2, 99.5, 61.1, 56.2, 56.1, 35.6, 31.6, 27.9, 22.2, 13.8. Anal. Calcd. For $C_{30}H_{32}FN_3O_5S$: C, 63.70; H, 5.70; N, 7.43. Found: C, 63.71; H, 5.72; N, 7.46. ESI-MS: m/z 566.2 $[M+H]^+$.

*4.1.4.8. N-(4-((6,7-Dimethoxyquinolin-4-yl)oxy)-3-fluorophenyl)-N'-((4-fluorobenzyl)sulfonyl)hexanamidine (**26h**)*

White solid, yield: 68%, m.p.: 152–154 °C. ^{1}H NMR (400 MHz, $CDCl_3$) δ 8.47 (d, J = 4.4 Hz, 1 H), 7.65 (d, J = 11.6 Hz, 1 H), 7.57 (s, 1 H), 7.51–7.38 (m, 3 H), 7.16 (s, 1 H), 7.01 (t, J = 8.0 Hz, 2 H), 6.83–6.76 (m, 1 H), 6.37 (d, J = 5.2 Hz, 1 H), 4.31 (s, 2 H), 4.04 (s, 3 H), 4.01 (s, 3 H), 2.26–2.17 (m, 2 H), 1.74–1.54 (m, 2 H), 1.25–1.24 (m, 4 H), 0.82 (t, J = 5.6 Hz, 3 H). ^{13}C NMR (100 MHz, $CDCl_3$) δ 168.0, 162.9 (d, J = 245.2 Hz), 160.1, 154.0 (d, J = 249.3 Hz), 153.2, 149.8, 148.4, 146.7, 137.9 (d, J = 13.9 Hz), 136.3 (d, J = 10.0 Hz), 132.5 (d, J = 7.6 Hz), 125.7, 123.4, 118.2, 115.6, 115.5 (d, J = 21.5 Hz), 111.9 (d, J = 23.2 Hz), 107.4, 102.2, 99.5, 60.2, 56.2, 56.1, 35.7, 31.6, 27.9, 22.2, 13.8. Anal. Calcd. For $C_{30}H_{31}F_2N_3O_5S$: C, 61.74; H, 5.35; N, 7.20. Found: C, 61.76; H, 5.35; N, 7.21. ESI-MS: m/z 606.2 $[M+Na]^+$.

*4.1.4.9. N'-(Benzylsulfonyl)-N-(4-((6,7-dimethoxyquinolin-4-yl)oxy)-3-fluorophenyl)-2-phenylacetamidine (**26i**)*

Light yellow solid, yield: 54%, m.p.: 104–106 °C. ^{1}H NMR (400 MHz, $CDCl_3$) δ 8.47 (d, J = 4.8 Hz, 1 H), 7.55 (s, 1 H), 7.48–7.47 (m, 3 H), 7.41 (s, 2 H), 7.40–7.27 (m, 6 H), 7.12 (t, J = 8.4 Hz, 1 H), 6.86–6.82 (m, 2 H), 6.33 (d, J = 5.2 Hz, 1 H), 4.40 (s, 2 H), 4.36 (s, 2 H), 4.05 (s, 3 H), 4.03 (s, 3 H). ^{13}C NMR (100 MHz, $CDCl_3$) δ 164.8, 159.9, 154.0 (d, J = 249.3 Hz), 153.1, 149.8, 148.5, 146.8, 138.4 (d, J = 13.4 Hz), 135.3 (d, J = 8.6 Hz), 132.8, 130.9, 130.0, 129.8, 129.6, 128.6, 128.5, 128.4, 123.5, 118.3, 115.5, 111.9 (d, J = 22.7 Hz), 107.7, 102.2, 99.3, 61.1, 56.2, 56.1, 40.6. Anal. Calcd. For $C_{32}H_{28}FN_3O_5S$: C, 65.63; H, 4.82; N, 7.18. Found: C, 65.64; H, 4.81; N, 7.20. ESI-MS: m/z 586.2 $[M+H]^+$.

*4.1.4.10. N-(4-((6,7-Dimethoxyquinolin-4-yl)oxy)-3-fluorophenyl)-N'-((4-fluorobenzyl)sulfonyl)-2-phenylacetamidine (**26j**)*

Light yellow solid, yield: 62%, m.p.: 93–95 °C. ^{1}H NMR (400 MHz, $CDCl_3$) δ 8.47 (d, J = 5.2 Hz, 1 H), 7.55 (s, 1 H), 7.51 (d, J = 11.6 Hz, 1 H), 7.45–7.42 (m, 5 H), 7.28 (d, J = 6.4 Hz, 2 H), 7.14 (t, J = 8.4 Hz, 1 H), 7.05 (t, J = 8.4 Hz, 2 H), 6.93–6.80 (m,

2 H), 6.33 (d, *J* = 4.8 Hz, 1 H), 4.39 (s, 2 H), 4.36 (s, 2 H), 4.05 (s, 3 H), 4.04 (s, 3 H). ^{13}C NMR (100 MHz, $CDCl_3$) δ 164.8, 164.1, 161.7, 161.1 (d, *J* = 247.0 Hz), 154.0 (d, *J* = 248.7 Hz), 153.1, 149.8, 148.5, 146.9, 138.5 (d, *J* = 12.8 Hz), 135.2 (d, *J* = 9.6 Hz), 132.8, 132. 6 (d, *J* = 8.2 Hz), 129.9, 129.6, 128.4, 125.7, 123.5, 118.3, 115.6 (d, *J* = 21.5 Hz), 112.0 (d, *J* = 22.4 Hz), 107.6, 102.2, 99.4, 60.1, 56.2, 56.1, 40.6. Anal. Calcd. For $C_{32}H_{27}F_2N_3O_5S$: C, 63.67; H, 4.51; N, 6.96. Found: C, 63.69; H, 4.52; N, 6.97. ESI-MS: *m*/*z* 603.2 $[M]^+$.

*4.1.4.11. N'-(Benzylsulfonyl)-N-(4-((6,7-dimethoxyquinolin-4-yl)oxy)-3-fluorophenyl)-(3-methoxy)propanamidine (**26k**)*

Yellow solid, yield: 73%, m.p.: 148–150 °C. ^{1}H NMR (400 MHz, $CDCl_3$) δ 8.85 (br s, 1 H), 8.51 (d, *J* = 5.2 Hz, 1 H), 7.61 (dd, *J* = 2.4, 12.0 Hz, 1 H), 7.58 (s, 1 H), 7.46–7.44 (m, 3 H), 7.37–7.32 (m, 3 H), 7.19 (t, *J* = 8.4 Hz, 1 H), 7.05–7.03 (m, 1 H), 6.38 (d, *J* = 5.2 Hz, 1 H), 4.35 (s, 2 H), 4.07 (s, 3 H), 4.05 (s, 3 H), 3.70 (t, *J* = 5.2 Hz, 2 H), 3.44 (s, 3 H), 3.21 (t, *J* = 5.2 Hz, 2 H). ^{13}C NMR (100 MHz, $CDCl_3$) δ 165.4, 160.0, 154.1 (d, *J* = 248.8 Hz), 153.0, 149.7, 148.6, 146.8, 138.0 (d, *J* = 12.3 Hz), 135.8 (d, *J* = 9.3 Hz), 130.8, 129.8, 128.6, 128.4, 123.5, 118.1 (d, *J* = 3.2 Hz), 115.5, 111.7 (d, *J* = 22.6 Hz), 107.7, 102.2, 99.4, 68.8, 60.9, 58.9, 56.2, 56.1, 33.9. Anal. Calcd. For $C_{28}H_{28}FN_3O_6S$: C, 60.75; H, 5.10; N, 7.59. Found: C, 60.73; H, 5.12; N, 7.60. ESI-MS: *m*/*z* 554.2 $[M+H]^+$.

*4.1.4.12. N-(4-((6,7-Dimethoxyquinolin-4-yl)oxy)-3-fluorophenyl)-N'-((4-fluorobenzyl)sulfonyl)-(3-methoxy)propanamidine (**26l**)*

Yellow solid, yield: 76%, m.p.: 145–147 °C. ^{1}H NMR (400 MHz, $CDCl_3$) δ 8.89 (br s, 1 H), 8.51 (d, *J* = 5.2 Hz, 1 H), 7.63 (dd, *J* = 1.6, 12.0 Hz, 1 H), 7.58 (s, 1 H), 7.44 (s, 2 H), 7.42–7.40 (m, 1 H), 7.20 (t, *J* = 8.4 Hz, 1 H), 7.06–7.02 (m, 3 H), 6.38 (d, *J* = 5.2 Hz, 1 H), 4.32 (s, 2 H), 4.07 (s, 3 H), 4.05 (s, 3 H), 3.73 (t, *J* = 5.2 Hz, 2 H), 3.45 (s, 3 H), 3.24 (t, *J* = 4.8 Hz, 2 H). ^{13}C NMR (100 MHz, $CDCl_3$) δ 165.4, 162.9 (d, *J* = 246.2 Hz), 159.9, 154.1 (d, *J* = 248.4 Hz), 153.0, 149.7, 148.6, 146.9, 138.1 (d, *J* = 12.4 Hz), 135.7 (d, *J* = 9.3 Hz), 132.5 (d, *J* = 8.2 Hz), 125.7 (d, *J* = 3.0 Hz), 123.5, 118.1 (d , *J* = 2.9 Hz), 115.6 (d, *J* = 21.5 Hz), 111.8 (d, *J* = 22.8 Hz), 107.7, 102.2, 99.3, 68.8, 60.0, 58.9, 56.2, 56.1, 34.0. Anal. Calcd. For $C_{28}H_{27}F_2N_3O_6S$: C, 58.84; H, 4.76; N, 7.35. Found: C, 58.87; H, 4.75; N, 7.37. ESI-MS: *m*/*z* 572.3 $[M+H]^+$.

*4.1.4.13. N'-(Benzylsulfonyl)-N-(4-((6,7-dimethoxyquinolin-4-yl)oxy)-3-fluorophenyl)acetamidine (**26m**)*

Light yellow solid, yield: 46%, m.p.: 126–128 °C. ^{1}H NMR (400 MHz, $CDCl_3$) δ 8.75 (br s, 1 H), 8.46 (d, *J* = 5.2 Hz, 1 H), 7.64 (d, *J* = 11.6 Hz, 1 H), 7.57 (s, 1 H), 7.50–7.43 (m, 3 H), 7.38 (s, 1 H), 7.35–7.32 (m, 2 H), 7.20–7.11 (m, 2 H), 6.38 (d, *J* = 4.8 Hz, 1 H), 4.35 (s, 2 H), 4.04 (s, 3 H), 4.01 (s, 3 H), 2.46 (s, 3 H). ^{13}C NMR (100 MHz, $CDCl_3$) δ 164.3, 160.2, 154.0 (d, *J* = 248.4 Hz), 153.2, 149.8, 148.4, 146.6, 138.0 (d, *J* = 12.3 Hz), 136.1 (d, *J* = 9.2 Hz), 130.9, 129.6, 128.7, 128.6, 123.5, 118.2 (d, *J* = 3.1 Hz), 115.6, 111.7 (d, *J* = 22.6 Hz), 107.3, 102.3, 99.5, 61.0, 56.2, 21.9. Anal. Calcd. For $C_{26}H_{24}FN_3O_5S$: C, 61.29; H, 4.75; N, 8.25. Found: C, 61.30; H, 4.77; N, 8.24. ESI-MS: *m*/*z* 532.2 $[M+Na]^+$.

*4.1.4.14. N-(4-((6,7-Dimethoxyquinolin-4-yl)oxy)-3-fluorophenyl)-N'-((4-fluorobenzyl)sulfonyl)acetamidine (**26n**)*

Light yellow solid, yield: 49%, m.p.: 119–121 °C. ^{1}H NMR (400 MHz, $CDCl_3$) δ 8.68 (br s, 1 H), 8.48 (d, J = 5.2 Hz, 1 H), 7.65 (d, J = 12.0 Hz, 1 H), 7.57 (s, 1 H), 7.43–7.40 (m, 2 H), 7.38 (s, 1 H), 7.18–7.11 (m, 2 H), 7.03 (t, J = 8.4 Hz, 2 H), 6.38 (d, J = 4.8 Hz, 1 H), 4.32 (s, 2 H), 4.05 (s, 3 H), 4.02 (s, 3 H), 2.53 (s, 3 H). ^{13}C NMR (100 MHz, $CDCl_3$) δ 164.3, 163.0 (d, J = 247.1 Hz), 160.1, 154.0 (d, J = 248.0 Hz), 153.3, 149.9, 148.5, 146.7, 138.2 (d, J = 12.7 Hz), 136.0 (d, J = 9.5 Hz), 132.6 (d, J = 8.0 Hz), 125.6 (d, J = 3.3 Hz), 123.5, 118.2, 115.7 (d, J = 21.5 Hz), 115.6, 111.8 (d, J = 22.7 Hz), 107.4, 102.3, 99.5, 60.1, 56.2, 22.0. Anal. Calcd. For $C_{26}H_{23}F_2N_3O_5S$: C, 59.20; H, 4.39; N, 7.97. Found: C, 59.21; H, 4.37; N, 7.94. ESI-MS: m/z 528.1 $[M+H]^+$.

*4.1.4.15. N'-(Benzylsulfonyl)-2-(cyclohexen-1-yl)-N-(4-((6,7-dimethoxyquinolin-4-yl)oxy)-3-fluorophenyl)acetamidine (**26o**)*

White solid, yield: 68%, m.p.: 141–143 °C. ^{1}H NMR (400 MHz, $CDCl_3$) δ 8.50 (d, J = 4.4 Hz, 1 H), 7.60–7.58 (m, 2 H), 7.47 (d, J = 11.6 Hz, 2 H), 7.44–7.43 (m, 2 H), 7.37–7.33 (m, 3 H), 7.19 (t, J = 8.4 Hz, 1 H), 7.02–7.00 (m, 1 H), 6.38 (d, J = 4.8 Hz, 1 H), 4.36 (s, 2 H), 4.06 (s, 3 H), 4.04 (s, 3 H), 3.63 (s, 2 H), 2.13–2.10 (m, 2 H), 1.95–1.94 (m, 2 H), 1.65–1.60 (m, 4 H). ^{13}C NMR (100 MHz, $CDCl_3$) δ 164.6, 159.9, 154.2 (d, J = 249.0 Hz), 153.1, 149.8, 148.7, 147.0, 138.4 (d, J = 12.5 Hz), 135.4 (d, J = 9.2 Hz), 132.1, 130.9, 130.7, 129.9, 128.6, 128.5, 123.6, 117.9 (d, J = 2.8 Hz), 115.6, 111.7 (d, J = 22.6 Hz), 107.8, 102.3, 99.4, 61.0, 56.2, 43.0, 28.5, 25.5, 22.7, 21.8. Anal. Calcd. For $C_{32}H_{32}FN_3O_5S$: C, 65.18; H, 5.47; N, 7.13. Found: C, 65.17; H, 5.49; N, 7.13. ESI-MS: m/z 590.2 $[M+H]^+$.

*4.1.4.16. 2-(Cyclohexen-1-yl)-N-(4-((6,7-dimethoxyquinolin-4-yl)oxy)-3-fluorophenyl)-N'-((4-fluorobenzyl)sulfonyl)acetamidine (**26p**)*

White solid, yield: 71%, m.p.: 132–134 °C. ^{1}H NMR (400 MHz, $CDCl_3$) δ 8.50 (d, J = 4.8 Hz, 1 H), 7.61 (dd, J = 1.6, 12.0 Hz, 1 H), 7.57 (s, 1 H), 7.51 (s, 1 H), 7.43–7.40 (m, 3 H), 7.21 (t, J = 8.4 Hz, 1 H), 7.06–6.98 (m, 3 H), 6.37 (d, J = 4.8 Hz, 1 H), 4.32 (s, 2 H), 4.07 (s, 3 H), 4.04 (s, 3 H), 3.66 (s, 2 H), 2.14–2.10 (m, 2 H), 1.97–1.95 (m, 2 H), 1.66–1.60 (m, 4 H). ^{13}C NMR (100 MHz, $CDCl_3$) δ 164.7, 163.0 (d, J = 246.4 Hz), 159.9, 154.2 (d, J = 249.4 Hz), 153.1, 149.8, 148.7, 147.0, 138.5 (d, J = 12.2 Hz), 135.3 (d, J = 8.6 Hz), 132.6 (d, J = 8.2 Hz), 132.0, 130.8, 125.8 (d, J = 2.5 Hz), 123.7, 118.0, 115.6 (d, J = 21.4 Hz), 111.8 (d, J = 23.0 Hz), 107.9, 102.2, 99.4, 60.2, 56.2, 43.1, 28.5, 25.5, 22.7, 21.8. Anal. Calcd. For $C_{32}H_{31}F_2N_3O_5S$: C, 63.25; H, 5.14; N, 6.91. Found: C, 63.26; H, 5.12; N, 6.92. ESI-MS: m/z 630.2 $[M+Na]^+$.

*4.1.4.17. N'-(Benzylsulfonyl)-N-(4-((6,7-dimethoxyquinolin-4-yl)oxy)-3-fluorophenyl)-2-(pyridin-3-yl)acetamidine (**26q**)*

Yellow solid, yield: 42%, m.p.: 121–123 °C. ^{1}H NMR (400 MHz, $CDCl_3$) δ 8.51 (s, 1 H), 8.46 (d, J = 4.8 Hz, 1 H), 8.17 (s, 1 H), 7.70 (d, J = 7.2 Hz, 1 H), 7.58 (d, J = 12.0 Hz, 1 H), 7.55 (s, 1 H), 7.46–7.45 (m, 2 H), 7.39 (s, 1 H), 7.36–7.29 (m, 4 H), 7.14 (t, J = 8.4 Hz, 1 H), 7.06–7.04 (m, 1 H), 6.66–6.62 (m, 1 H), 6.36 (d, J = 4.8 Hz, 1 H), 4.40 (s, 2 H), 4.24 (s, 2 H), 4.04 (s, 3 H), 4.02 (s, 3 H). ^{13}C NMR (100 MHz, $CDCl_3$) δ 163.5, 159.9, 154.1 (d, J = 248.1 Hz), 153.1, 150.1, 149.8, 148.6, 148.5, 146.9, 138.4 (d, J = 11.9 Hz), 137.5, 135.8 (d, J = 7.6 Hz), 131.0, 130.6, 129.6, 128.7, 124.4, 124.1, 123.6, 118.5, 115.6, 112.0 (d, J =

22.9 Hz), 107.7, 102.3, 99.4, 61.1, 56.2, 37.8. Anal. Calcd. For $C_{31}H_{27}FN_4O_5S$: C, 63.47; H, 4.64; N, 9.55. Found: C, 63.44; H, 4.66; N, 9.56. ESI-MS: *m*/*z* 587.2 $[M+H]^+$.

4.1.4.18. N-(4-((6,7-Dimethoxyquinolin-4-yl)oxy)-3-fluorophenyl)-N'-((4-fluorobenzyl)sulfonyl)-2-(pyridin-3-yl)acetamidine ***(26r)***

Yellow solid, yield: 44%, m.p.: 112–114 °C. ^{1}H NMR (400 MHz, $CDCl_3$) δ 8.51 (s, 1 H), 8.46 (d, *J* = 4.8 Hz, 1 H), 8.15 (s, 1 H), 7.74 (d, *J* = 7.2 Hz, 1 H), 7.61 (d, *J* = 12.0 Hz, 1 H), 7.55 (s, 1 H), 7.44–7.41 (m, 2 H), 7.38 (s, 1 H), 7.34 –7.31 (m, 1 H), 7.24–7.22 (m, 1 H), 7.15 (t, *J* = 8.4 Hz, 1 H), 7.06–7.03 (t, *J* = 8.0 Hz, 3 H), 6.35 (d, *J* = 4.8 Hz, 1 H), 4.37 (s, 2 H), 4.27 (s, 2 H), 4.04 (s, 3 H), 4.02 (s, 3 H). ^{13}C NMR (100 MHz, $CDCl_3$) δ 164.2, 163.6, 161.8, 159.9, 154.0 (d, *J* = 248.9 Hz), 153.1, 151.2 (d, *J* = 245.9 Hz), 149.8, 148.6, 146.9, 138.5 (d, *J* = 11.8 Hz), 137.4, 135.8 (d, *J* = 8.5 Hz), 132.7 (d, *J* = 8.1 Hz), 130.6, 125.5, 124.5, 123.6, 118.4, 115.7 (d, *J* = 21.5 Hz), 115.6, 112.1 (d, *J* = 21.8 Hz), 107.6, 102.3, 99.4, 60.2, 56.2, 37.9. Anal. Calcd. For $C_{31}H_{26}F_2N_4O_5S$: C, 61.58; H, 4.33; N, 9.27. Found: C, 61.60; H, 4.31; N, 9.30. ESI-MS: *m*/*z* 605.2 $[M+H]^+$.

4.1.4.19. N'-(Benzylsulfonyl)-N-(4-((6,7-dimethoxyquinolin-4-yl)oxy)-3-fluorophenyl)-2-(thien-3-yl)acetamidine ***(26s)***

Light yellow solid, yield: 62%, m.p.: 116–118 °C. ^{1}H NMR (400 MHz, $CDCl_3$) δ 8.48 (d, *J* = 5.2 Hz, 1 H), 7.55 (s, 1 H), 7.51 (d, *J* = 12.0 Hz, 1 H), 7.47–7.35 (m, 7 H), 7.16–7.12 (m, 2 H), 7.00 (d, *J* = 4.4 Hz, 1 H), 6.89–6.87 (m, 1 H), 6.34 (d, *J* = 5.2 Hz, 1 H), 4.39 (s, 2 H), 4.37 (s, 2 H), 4.05 (s, 3 H), 4.03 (s, 3 H). ^{13}C NMR (100 MHz, DMSO-d_6) δ 163.7, 159.1, 153.1 (d, *J* = 245.1 Hz), 152.6, 149.5, 148.8, 146.4, 136.9 (d, *J* = 12.1 Hz), 136.6 (d, *J* = 9.7 Hz), 134.7, 130.9, 130.5, 128.5, 128.1, 127.9, 126.1, 123.8, 123.3, 118.5 (d, *J* = 2.4 Hz), 114.5, 110.7 (d, *J* = 22.6 Hz), 107.8, 102.2, 98.9, 59.9, 55.7, 34.4. Anal. Calcd. For $C_{30}H_{26}FN_3O_5S_2$: C, 60.90; H, 4.43; N, 7.10. Found: C, 60.91; H, 4.45; N, 7.08. ESI-MS: *m*/*z* 614.2 $[M+Na]^+$.

4.1.4.20. N-(4-((6,7-Dimethoxyquinolin-4-yl)oxy)-3-fluorophenyl)-N'-((4-fluorobenzyl)sulfonyl)-2-(thien-3-yl)acetamidine ***(26t)***

Light yellow solid, yield: 56%, m.p.: 107–109 °C. ^{1}H NMR (400 MHz, $CDCl_3$) δ 8.47 (d, *J* = 4.0 Hz, 1 H), 7.55 (s, 1 H), 7.42–7.42 (m, 3 H), 7.40 (s, 1 H), 7.29–7.26 (m, 2 H), 7.15 (t, *J* = 8.4 Hz, 1 H), 7.04 (t, *J* = 8.4 Hz, 3 H), 6.88–6.86 (m, 1 H), 6.33 (d, *J*= 5.2 Hz, 1 H), 4.40 (s, 2 H), 4.34 (s, 2 H), 4.05 (s, 3 H), 4.02 (s, 3 H). ^{13}C NMR (100 MHz, $CDCl_3$) δ 164.4, 164.2, 161.7, 158.7 (d, *J* = 246.4 Hz), 154.0 (d, *J* = 248.7 Hz), 153.1, 149.8, 148.6, 146.8, 138.5 (d, *J* = 11.9 Hz), 135.2 (d, *J* = 8.8 Hz), 132.6 (d, *J* = 8.4 Hz), 132.5, 128.5, 127.9, 125.6 (d, *J* = 2.3 Hz), 125.5, 123.5, 118.3, 115.6 (d, *J* = 21.5 Hz), 111.9 (d, *J* = 22.5 Hz), 107.6, 102.2, 99.4, 60.1, 56.2, 35.2. Anal. Calcd. For $C_{30}H_{25}F_2N_3O_5S_2$: C, 59.10; H, 4.13; N, 6.89. Found: C, 59.09; H, 4.15; N, 6.90. ESI-MS: *m*/*z* 610.2 $[M+H]^+$.

4.1.4.21. N-(4-((6,7-Dimethoxyquinolin-4-yl)oxy)-3-fluorophenyl)-3-methoxy-N'-((2-methylbenzyl)sulfonyl)propanamidine ***(26u)***

Yellow solid, yield: 78%, m.p.: 115–117 °C. ^{1}H NMR (400 MHz, $CDCl_3$) δ 8.84 (br s, 1 H), 8.51 (d, *J* = 5.2 Hz, 1 H), 7.58 (s, 1 H), 7.56 (dd, *J* = 2.0, 12.0 Hz, 1 H), 7.43 (s, 1 H), 7.41 (d, *J* = 7.2 Hz, 1 H), 7.22–7.16 (m, 4 H), 7.10–7.08 (m, 1 H), 6.39 (d, *J* = 5.2 Hz, 1 H), 4.42 (s, 2 H), 4.07 (s, 3 H), 4.05 (s, 3 H), 3.66 (t, *J* = 5.2 Hz, 2 H), 3.43 (s, 3 H), 3.17 (t, *J* = 5.2 Hz, 2 H), 2.41 (s,

3 H). ^{13}C NMR (100 MHz, $CDCl_3$) δ 165.7, 160.0, 154.1 (d, J = 249.0 Hz), 153.0, 149.7, 148.7, 147.0, 138.3 (d, J = 12.1 Hz), 138.2, 135.7 (d, J = 9.5 Hz), 131.8, 130.8, 128.7, 128.1, 126.1, 123.6, 118.4 (d, J = 3.1Hz), 115.5, 111.8 (d, J = 22.5 Hz), 107.8, 102.2, 99.4, 68.8, 58.9, 58.0, 56.2, 33.5, 20.0. Anal. Calcd. For$C_{29}H_{30}FN_3O_6S$: C, 61.36; H, 5.33; N, 7.40. Found: C, 61.37; H, 5.33; N, 7.42. ESI-MS: m/z 568.2 $[M+H]^+$.

*4.1.4.22. N-(4-((6,7-Dimethoxyquinolin-4-yl)oxy)-3-fluorophenyl)-3-methoxy-N'-((3-methylbenzyl)sulfonyl)propanamidine (**26v**)*

Yellow solid, yield: 72%, m.p.: 124–126 °C. ^{1}H NMR (400 MHz, $CDCl_3$) δ 8.87 (br s, 1 H), 8.50 (d, J = 5.2 Hz, 1 H), 7.65 (dd, J = 2.0, 11.6 Hz, 1 H), 7.58 (s, 1 H), 7.43 (s, 1 H), 7.27 (s, 1 H), 7.24–7.23 (m, 2 H), 7.18 (t, J = 8.8 Hz, 1 H), 7.13 (t, J = 3.6 Hz, 1 H), 7.08–7.06 (m, 1 H), 6.38 (d, J = 5.2 Hz, 1 H), 4.32 (s, 2 H), 4.06 (s, 3 H), 4.05 (s, 3 H), 3.69 (t, J = 5.2 Hz, 2 H), 3.44 (s, 3 H), 3.22 (t, J = 5.2 Hz, 2 H), 2.31 (s, 3 H). ^{13}C NMR (100 MHz, $CDCl_3$) δ 165.4, 159.9, 154.1 (d, J = 248.9 Hz), 153.0, 149.7, 148.7, 146.9, 138.3, 138.0 (d, J = 12.2 Hz), 135.8 (d, J = 9.4 Hz), 131.5, 129.6, 129.3, 128.5, 128.0, 123.5, 118.0 (d, J = 3.0 Hz), 115.5, 111.6 (d, J = 22.9 Hz), 107.8, 102.3, 99.4, 68.8, 60.9, 58.9, 56.2, 33.8, 21.3. Anal. Calcd. For $C_{29}H_{30}FN_3O_6S$: C, 61.36; H, 5.33; N, 7.40. Found: C, 61.35; H, 5.31; N, 7.43. ESI-MS: m/z 568.2 $[M+H]^+$.

*4.1.4.23. N-(4-((6,7-Dimethoxyquinolin-4-yl)oxy)-3-fluorophenyl)-3-methoxy-N'-((4-methylbenzyl)sulfonyl)propanamidine (**26w**)*

Yellow solid, yield: 82%, m.p.: 129–131 °C. ^{1}H NMR (400 MHz, $CDCl_3$) δ 8.85 (br s, 1 H), 8.51 (d, J = 5.2 Hz, 1 H), 7.64 (dd, J = 2.4, 12.0 Hz, 1 H), 7.59 (s, 1 H), 7.44 (s, 1 H), 7.33 (d, J = 7.6 Hz, 2 H), 7.21–7.15 (m, 3 H), 7.06–7.04 (m, 1 H), 6.39 (d, J = 5.2 Hz, 1 H), 4.31 (s, 2 H), 4.07 (s, 3 H), 4.05 (s, 3 H), 3.69 (t, J = 5.2 Hz, 2 H), 3.44 (s, 3 H), 3.22 (t, J = 5.2 Hz, 2 H), 2.31 (s, 3 H). ^{13}C NMR (100 MHz, $CDCl_3$) δ 165.4, 160.0, 154.1 (d, J = 248.5 Hz), 153.0, 149.7, 148.7, 146.9, 138.4, 138.1 (d, J = 12.5 Hz), 135.8 (d, J = 9.3 Hz), 130.7, 129.3, 126.7, 123.5, 118.1 (d, J = 3.2 Hz), 115.5, 111.7 (d, J = 22.7 Hz), 107.8, 102.2, 99.4, 68.8, 60.7, 58.9, 56.2, 33.8, 21.2. Anal. Calcd. For $C_{29}H_{30}FN_3O_6S$: C, 61.36; H, 5.33; N, 7.40. Found: C, 61.38; H, 5.34; N, 7.43. ESI-MS: m/z 590.2 $[M+Na]^+$.

*4.1.4.24. N-(4-((6,7-Dimethoxyquinolin-4-yl)oxy)-3-fluorophenyl)-N'-((2-fluorobenzyl)sulfonyl)-3-methoxypropanamidine (**26x**)*

Yellow solid, yield: 71%, m.p.: 137–139 °C. ^{1}H NMR (400 MHz, $CDCl_3$) δ 8.89 (br s, 1 H), 8.51 (d, J = 5.2 Hz, 1 H), 7.59 (s, 1 H), 7.58–7.57 (m, 1 H), 7.55 (dd, J = 1.6, 7.2 Hz, 1 H), 7.44 (s, 1 H), 7.32–7.28 (m, 1 H), 7.21–7.13 (m, 2 H), 7.08–7.06 (m, 2 H), 6.39 (d, J = 5.2 Hz, 1 H), 4.44 (s, 2 H), 4.07 (s, 3 H), 4.04 (s, 3 H), 3.73 (t, J = 5.2 Hz, 2 H), 3.45 (s, 3 H), 3.25 (t, J = 5.2 Hz, 2 H). ^{13}C NMR (100 MHz, $CDCl_3$) δ 165.5, 161.2 (d, J = 247.4 Hz), 160.0, 154.1 (d, J = 248.7 Hz), 153.0, 149.7, 148.7, 146.9, 138.2 (d, J = 12.5 Hz), 135.7 (d, J = 9.4 Hz), 132.6 (d, J = 2.3 Hz), 130.4 (d, J = 8.3 Hz), 124.3 (d, J = 3.6 Hz), 123.5, 118.2 (d, J = 3.0 Hz), 117.4 (d, J = 14.4 Hz), 115.7 (d, J = 21.7 Hz), 115.5, 111.7 (d, J = 22.7 Hz), 107.8, 102.3, 99.4, 68.6, 59.0, 56.2, 53.5, 33.9. Anal. Calcd. For $C_{28}H_{27}F_2N_3O_6S$: C, 58.84; H, 4.76; N, 7.35. Found: C, 58.85; H, 4.78; N, 7.35. ESI-MS: m/z 572.2

*4.1.4.25. N-(4-((6,7-Dimethoxyquinolin-4-yl)oxy)-3-fluorophenyl)-N'-((3-fluorobenzyl)sulfonyl)-3-methoxypropanamidine (**26y**)*

Yellow solid, yield: 68%, m.p.: 134–136 °C. ^{1}H NMR (400 MHz, $CDCl_3$) δ 8.90 (br s, 1 H), 8.51 (d, J = 5.2 Hz, 1 H), 7.58 (s,

1 H), 7.53 (dd, *J* = 2.4, 12.0 Hz, 1 H), 7.43 (s, 1 H), 7.34–7.29 (m, 1 H), 7.22–7.15 (m, 3 H), 7.07–7.01 (m, 2 H), 6.39 (d, *J* = 5.2 Hz, 1 H), 4.33 (s, 2 H), 4.06 (s, 3 H), 4.04 (s, 3 H), 3.73 (t, *J* = 5.2 Hz, 2 H), 3.45 (s, 3 H), 3.25 (t, *J* = 5.2 Hz, 2 H). ^{13}C NMR (100 MHz, $CDCl_3$) δ 165.5, 162.6 (d, *J* = 245.1 Hz), 159.9, 154.1 (d, *J* = 248.8 Hz), 153.0, 149.7, 148.7, 146.9, 138.3 (d, *J* = 12.3 Hz), 135.6 (d, *J* = 9.3 Hz), 132.1 (d, *J* = 8.0 Hz), 130.1 (d, *J* = 8.1 Hz), 126.6 (d, *J* = 2.6 Hz), 123.6, 118.4 (d, *J* = 3.3 Hz), 117.8 (d, *J* = 22.0 Hz), 115.6 (d, *J* = 7.1 Hz), 115.4, 111.7 (d, *J* = 22.6 Hz), 107.8, 102.3, 99.4, 68.8, 60.4, 59.0, 56.2, 33.9. Anal. Calcd. For $C_{28}H_{27}F_2N_3O_6S$: C, 58.84; H, 4.76; N, 7.35. Found: C, 58.83; H, 4.78; N, 7.36. ESI-MS: *m*/*z* 572.2 $[M+H]^+$.

*4.1.4.26. N'-((4-Chlorobenzyl)sulfonyl)-N-(4-((6,7-dimethoxyquinolin-4-yl)oxy)-3-fluorophenyl)-3-methoxypropanamidine (**26z**)*

Yellow solid, yield: 76%, m.p.: 146–148 °C. ^{1}H NMR (400 MHz, $CDCl_3$) δ 8.90 (br s, 1 H), 8.52 (d, *J* = 5.2 Hz, 1 H), 7.62 (dd, *J* = 2.4, 12.0 Hz, 1 H), 7.58 (s, 1 H), 7.43 (s, 1 H), 7.38 (d, *J* = 8.4 Hz, 2 H), 7.32 (d, *J* = 8.4 Hz, 2 H), 7.20 (t, *J* = 8.4 Hz, 1 H), 7.03-7.01 (m, 1 H), 6.39 (d, *J* = 5.2 Hz, 1 H), 4.31 (s, 2 H), 4.07 (s, 3 H), 4.05 (s, 3 H), 3.72 (t, *J* = 5.2 Hz, 2 H), 3.45 (s, 3 H), 3.24 (t, *J* = 5.2 Hz, 2 H). ^{13}C NMR (100 MHz, $CDCl_3$) δ 165.5, 159.9, 154.1 (d, *J* = 248.2 Hz), 153.0, 149.8, 148.8, 146.9, 138.3 (d, *J* = 12.3 Hz), 135.6 (d, *J* = 10.0 Hz), 134.7, 132.2, 128.8, 128.4, 123.6, 118.2, 115.5, 111.9 (d, *J* = 22.6 Hz), 107.9 (d, *J* = 3.4 Hz), 102.3, 99.4, 68.8, 60.2, 59.0, 56.2, 34.0. Anal. Calcd. For $C_{28}H_{27}ClFN_3O_6S$: C, 57.19; H, 4.63; N, 7.15. Found: C, 57.22; H, 4.62; Cl, 6.03; N, 7.18. ESI-MS: *m*/*z* 588.2 $[M+H]^+$.

*4.1.4.27. N'-((4-Bromobenzyl)sulfonyl)-N-(4-((6,7-dimethoxyquinolin-4-yl)oxy)-3-fluorophenyl)-3-methoxypropanamidine (**26aa**)*

Yellow solid, yield: 82%, m.p.: 151–153 °C. ^{1}H NMR (400 MHz, $CDCl_3$) δ 8.90 (br s, 1 H), 8.53 (d, *J* = 4.8 Hz, 1 H), 7.62 (dd, *J* = 2.0, 11.6 Hz, 1 H), 7.59 (s, 1 H), 7.49 (s, 1 H), 7.45 (d, *J* = 8.0 Hz, 2 H), 7.31 (d, *J* = 8.0 Hz, 2 H), 7.20 (t, *J* = 8.4 Hz, 1 H), 7.03–7.00 (m, 1 H), 6.39 (d, *J* = 5.2 Hz, 1 H), 4.29 (s, 2 H), 4.07 (s, 3 H), 4.05 (s, 3 H), 3.72 (t, *J* = 5.2 Hz, 2 H), 3.45 (s, 3 H), 3.24 (t, *J* = 5.2 Hz, 2 H). ^{13}C NMR (100 MHz, $CDCl_3$) δ 165.5, 159.9, 154.1 (d, *J* = 248.4 Hz), 153.1, 149.8, 148.8, 146.9, 138.3 (d, *J* = 12.3 Hz), 135.6 (d, *J* = 9.3 Hz), 132.5, 131.8, 128.9, 123.6, 122.9, 118.2 (d, *J* = 3.2 Hz), 115.6, 111.9 (d, *J* = 22.8 Hz), 107.9, 102.3, 99.4, 68.8, 60.3, 59.0, 56.2, 33.9. Anal. Calcd. For $C_{28}H_{27}BrFN_3O_6S$: C, 53.17; H, 4.30; N, 6.64. Found: C, 53.20; H, 4.31; N, 6.65. ESI-MS: *m*/*z* 654.1 $[M+Na]^+$.

*4.1.4.28. N'-((3,4-Dichlorobenzyl)sulfonyl)-N-(4-((6,7-dimethoxyquinolin-4-yl)oxy)-3-fluorophenyl)-3-methoxypropanamidine (**26ab**)*

Yellow solid, yield: 71%, m.p.: 135–137 °C. ^{1}H NMR (400 MHz, $CDCl_3$) δ 8.93 (br s, 1 H), 8.51 (d, *J* = 5.2 Hz, 1 H), 7.58 (s, 1 H), 7.55 (dd, *J* = 2.4, 12.0 Hz, 1 H), 7.52 (d, *J* = 2.0 Hz, 1 H), 7.43 (s, 1 H), 7.41 (d, *J* = 8.4 Hz, 1 H), 7.27 (dd, *J* = 2.0, 8.0 Hz, 1 H), 7.22 (d, *J* = 8.8 Hz, 1 H), 7.09–7.07 (m, 1 H), 6.41 (d, *J* = 5.2 Hz, 1 H), 4.27 (s, 2 H), 4.07 (s, 3 H), 4.05 (s, 3 H), 3.74 (t, *J* = 5.6 Hz, 2 H), 3.46 (s, 3 H), 3.25 (t, *J* = 5.6 Hz, 2 H). ^{13}C NMR (100 MHz, $CDCl_3$) δ 165.7, 159.9, 154.1 (d, *J* = 249.0 Hz), 153.1, 149.8, 148.7, 147.0, 138.5 (d, *J* = 12.5 Hz), 135.4 (d, *J* = 9.3 Hz), 132.9, 132.7, 132.6, 130.5, 130.2, 130.1, 123.6, 118.5 (d, *J* = 3.1 Hz), 115.6, 111.8 (d, *J* = 22.6 Hz), 107.8, 102.4, 99.4, 68.7, 59.7, 59.0, 56.2, 34.0. Anal. Calcd. For $C_{28}H_{26}Cl_2FN_3O_6S$: C,

54.02; H, 4.21; N, 6.75. Found: C, 54.04; H, 4.20; N, 6.77. ESI-MS: *m*/*z* 622.1 $[M+H]^+$.

4.1.4.29.

N-(4-((6,7-Dimethoxyquinolin-4-yl)oxy)-3-fluorophenyl)-3-methoxy-N'-((4-(trifluoromethyl)benzyl)sulfonyl)propanamidine

(26ac)

Yellow solid, yield: 54%, m.p.: 154–156 °C. ^{1}H NMR (400 MHz, $CDCl_3$) δ 8.92 (br s, 1 H), 8.51 (d, *J* = 5.2 Hz, 1 H), 7.62–7.56 (m, 6 H), 7.44 (s, 1 H), 7.20 (t, *J* = 8.4 Hz, 1 H), 7.01–6.99 (m, 1 H), 6.38 (d, *J* = 5.2 Hz, 1 H), 4.39 (s, 2 H), 4.07 (s, 3 H), 4.05 (s, 3 H), 3.73 (t, *J* = 5.2 Hz, 2 H), 3.45 (s, 3 H), 3.25 (t, *J* = 5.2 Hz, 2 H). ^{13}C NMR (100 MHz, $CDCl_3$) δ 165.6, 159.9, 154.1 (d, *J* = 248.4 Hz), 153.1, 149.8, 148.7, 147.0, 138.4 (d, *J* = 12.4 Hz), 135.5 (d, *J* = 9.2 Hz), 133.9, 131.2, 130.7 (q, *J* = 32.4 Hz), 125.6 (q, *J* = 3.7 Hz), 124.0 (q, *J* = 270.6 Hz), 123.6, 118.3 (d, *J* = 3.3 Hz), 115.6, 112.0 (d, *J* = 22.7 Hz), 107.9, 102.2, 99.4, 68.7, 60.5, 59.0, 56.2, 34.0. Anal. Calcd. For $C_{29}H_{27}F_4N_3O_6S$: C, 56.03; H, 4.38; N, 6.76. Found: C, 56.04; H, 4.37; N, 6.78. ESI-MS: *m*/*z* 644.2 $[M+Na]^+$.

4.1.4.30. N-(4-((7-Butoxy-6-methoxyquinolin-4-yl)oxy)-3-fluorophenyl)-N'-((4-chlorobenzyl)sulfonyl)-3-methoxypropanamidine

(26ad)

Yellow solid, yield: 68%, m.p.: 115–117 °C. ^{1}H NMR (400 MHz, $CDCl_3$) δ 8.91 (br s, 1 H), 8.50 (d, *J* = 5.2 Hz, 1 H), 7.62 (dd, *J* = 2.4, 12.0 Hz, 1 H), 7.57 (s, 1 H), 7.43 (s, 1 H), 7.38 (d, *J* = 8.0 Hz, 2 H), 7.32 (d, *J* = 8.0 Hz, 2 H), 7.19 (t, *J* = 8.4 Hz, 1 H), 7.02–7.00 (m, 1 H), 6.37 (d, *J* = 5.2 Hz, 1 H), 4.30 (s, 2 H), 4.20 (t, *J* = 6.4 Hz, 2 H), 4.05 (s, 3 H), 3.72 (t, *J* = 5.2 Hz, 2 H), 3.45 (s, 3 H), 3.24 (t, *J* = 5.2 Hz, 2 H), 1.97–1.89 (m, 2 H), 1.59–1.50 (m, 2 H), 1.00 (t, *J* = 7.2 Hz, 3 H). ^{13}C NMR (100 MHz, $CDCl_3$) δ 165.5, 159.9, 154.1 (d, *J* = 248.6 Hz), 152.6, 150.1, 148.6, 146.9, 138.3 (d, *J* = 12.3 Hz), 135.6 (d, *J* = 9.4 Hz), 134.7, 132.2, 128.8, 128.4, 123.6, 118.2 (d, *J* = 2.9 Hz), 115.4, 111.9 (d, *J* = 22.8 Hz), 108.5, 102.1, 99.4, 68.8, 60.2, 59.0, 56.2, 34.0, 30.8, 19.3, 13.9. Anal. Calcd. For $C_{31}H_{33}ClFN_3O_6S$: C, 59.09; H, 5.28; N, 6.67. Found: C, 59.10; H, 5.30; N, 6.65. ESI-MS: *m*/*z* 630.2 $[M+H]^+$.

4.1.4.31.

N-(4-((7-Butoxy-6-methoxyquinolin-4-yl)oxy)-3-fluorophenyl)-N'-((3,4-dichlorobenzyl)sulfonyl)-3-methoxypropanamidine ***(26ae)***

Yellow solid, yield: 61%, m.p.: 107–109 °C. ^{1}H NMR (400 MHz, $CDCl_3$) δ 8.94 (br s, 1 H), 8.50 (d, *J* = 5.2 Hz, 1 H), 7.56 (s, 1 H), 7.55–7.51 (m, 2 H), 7.42–7.40 (m, 2 H), 7.28–7.26 (m, 1 H), 7.23 (t, *J* = 8.4 Hz, 1 H), 7.08–7.06 (m, 1 H), 6.39 (d, *J* = 5.2 Hz, 1 H), 4.27 (s, 2 H), 4.20 (t, *J* = 6.8 Hz, 2 H), 4.05 (s, 3 H), 3.74 (t, *J* = 5.2 Hz, 2 H), 3.46 (s, 3 H), 3.25 (t, *J* = 5.2 Hz, 2 H), 1.96–1.89 (m, 2 H), 1.59–1.50 (m, 2 H), 1.00 (t, *J* = 7.2 Hz, 3 H). ^{13}C NMR (100 MHz, $CDCl_3$) δ 165.6, 159.9, 154.1 (d, *J* = 248.9 Hz), 152.6, 150.1, 148.6, 146.9, 138.5 (d, *J* = 12.2 Hz), 135.4 (d, *J* = 9.1 Hz), 132.9, 132.7, 132.6, 130.5, 130.2, 130.1, 123.6, 118.5 (d, *J* = 3.2 Hz), 115.4, 111.8 (d, *J* = 22.6 Hz), 108.5, 102.3, 99.4, 68.8, 68.7, 59.7, 59.0, 56.2, 34.0, 30.8, 19.3, 13.9. Anal. Calcd. For $C_{31}H_{32}Cl_2FN_3O_6S$: C, 56.03; H, 4.85; N, 6.32. Found: C, 56.04; H, 4.85; N, 6.35. ESI-MS: *m*/*z* 663.1 $[M]^+$.

4.1.4.32.

*N'-((4-Chlorobenzyl)sulfonyl)-N-(3-fluoro-4-((6-methoxy-7-(3-morpholinopropoxy)quinolin-4-yl)oxy)phenyl)-3-methoxypropanamidine (**26af**)*

Yellow solid, yield: 74%, m.p.: 122–124 °C. ^{1}H NMR (400 MHz, $CDCl_3$) δ 8.88 (br s, 1 H), 8.50 (d, J = 5.2 Hz, 1 H), 7.62 (dd, J = 2.4, 12.0 Hz, 1 H), 7.57 (s, 1 H), 7.45 (s, 1 H), 7.38 (d, J = 8.4 Hz, 2 H), 7.32 (d, J = 8.4 Hz, 2 H), 7.20 (t, J = 8.4 Hz, 1 H), 7.02–7.01 (m, 1 H), 6.38 (d, J = 5.2 Hz, 1 H), 4.30 (s, 2 H), 4.27 (t, J = 6.4 Hz, 2 H), 4.05 (s, 3 H), 3.73–3.71 (m, 6 H), 3.45 (s, 3 H), 3.24 (t, J = 4.8 Hz, 2 H), 2.58 (t, J = 7.2 Hz, 2 H), 2.49–2.36 (m, 4 H), 2.17–2.10 (m, 2 H). ^{13}C NMR (100 MHz, $CDCl_3$) δ 165.5, 159.9, 154.1 (d, J = 248.5 Hz), 152.5, 150.0, 148.7, 146.9, 138.3 (d, J = 12.5 Hz), 135.6 (d, J = 9.3 Hz), 134.7, 132.2, 128.8, 128.4, 123.6, 118.2 (d, J = 3.2 Hz), 115.5, 111.9 (d, J = 22.6 Hz), 108.7, 102.2, 99.5, 68.8, 67.3, 67.0, 60.2, 59.0, 56.2, 55.4, 53.7, 33.9, 26.0. Anal. Calcd. For $C_{34}H_{38}ClFN_4O_7S$: C, 58.24; H, 5.46; N, 7.99. Found: C, 58.23; H, 5.47; N, 8.02. ESI-MS: *m/z* 723.2 $[M+Na]^+$.

4.1.4.33.

*N'-((3,4-Dichlorobenzyl)sulfonyl)-N-(3-fluoro-4-((6-methoxy-7-(3-morpholinopropoxy)quinolin-4-yl)oxy)phenyl)-3-methoxypropanamidine (**26ag**)*

Yellow solid, yield: 72%, m.p.: 110–112 °C. ^{1}H NMR (400 MHz, $CDCl_3$) δ 8.92 (br s, 1 H), 8.49 (d, J = 5.2 Hz, 1 H), 7.56 (s, 1 H), 7.55–7.51 (m, 2 H), 7.44 (s, 1 H), 7.41 (d, J = 8.0 Hz, 1 H), 7.28–7.26 (m, 1 H), 7.23 (t, J = 8.4 Hz, 1 H), 7.08–7.06 (m, 1 H), 6.39 (d, J = 5.2 Hz, 1 H), 4.28–4.25 (m, 4 H), 4.04 (s, 3 H), 3.75–3.71 (m, 6 H), 3.46 (s, 3 H), 3.25 (t, J = 5.2 Hz, 2 H), 2.58 (t, J = 7.2 Hz, 2 H), 2.50–2.48 (m, 4 H), 2.16–2.09 (m, 2 H). ^{13}C NMR (100 MHz, $CDCl_3$) δ 165.7, 159.8, 154.1 (d, J = 249.1 Hz), 152.5, 150.0, 148.6, 146.9, 138.5 (d, J = 12.2 Hz), 135.4 (d, J = 9.3 Hz), 132.9, 132.7, 132.6, 130.5, 130.2, 130.1, 123.6, 118.5 (d, J = 3.2 Hz), 115.5, 111.8 (d, J = 22.6 Hz), 108.7, 102.3, 99.5, 68.7, 67.3, 67.0, 59.7, 59.0, 56.2, 55.4, 53.7, 34.0, 26.0. Anal. Calcd. For $C_{34}H_{37}Cl_2FN_4O_7S$: C, 55.51; H, 5.07; N, 7.62. Found: C, 55.50; H, 5.09; N, 7.60. ESI-MS: *m/z* 757.2 $[M+Na]^+$.

4.1.4.34.

*N'-((4-Chlorobenzyl)sulfonyl)-N-(3-fluoro-4-((6-methoxy-7-(3-(piperidin-1-yl)propoxy)quinolin-4-yl)oxy)phenyl)-3-methoxypropanamidine (**26ah**)*

Yellow solid, yield: 64%, m.p.: 127–129 °C. ^{1}H NMR (400 MHz, $CDCl_3$) δ 9.26 (s, 1 H), 8.49 (d, J = 6.4 Hz, 1 H), 7.67 (dd, J = 2.0, 12.0 Hz, 1 H), 7.56 (s, 1 H), 7.39 (s, 1 H), 7.36 (d, J = 8.4 Hz, 2 H), 7.29 (d, J = 8.8 Hz, 2 H), 7.19–7.12 (m, 2 H), 6.37 (d, J = 4.8 Hz, 1 H), 4.30 (s, 2 H), 4.23 (t, J = 5.6 Hz, 2 H), 4.01 (s, 3 H), 3.74 (t, J = 5.2 Hz, 2 H), 3.41 (s, 3 H), 3.30–3.28 (m, 2 H), 3.23 (t, J = 5.6 Hz, 2 H), 2.99–2.95 (m, 2 H), 2.48–2.33 (m, 4 H), 1.76–1.73 (m, 2 H), 1.64–1.56 (m, 4 H). ^{13}C NMR (100 MHz, $CDCl_3$) δ 165.5, 160.1, 154.0 (d, J = 247.9 Hz), 151.8, 149.8, 148.9, 146.5, 138.0 (d, J = 12.4 Hz), 135.9 (d, J = 9.1 Hz), 134.6, 132.2, 128.8, 128.5, 123.5, 118.3 (d, J = 2.8 Hz), 115.8, 111.8 (d, J = 22.7 Hz), 109.7, 102.4, 99.7, 68.9, 66.3, 60.2, 59.0, 56.1,

55.3, 53.7, 34.1, 24.0, 23.2, 22.4. Anal. Calcd. For $C_{35}H_{40}ClFN_4O_6S$: C, 60.12; H, 5.77; N, 8.01. Found: C, 60.10; H, 5.78; N, 8.03. ESI-MS: *m*/*z* 699.3 $[M+H]^+$.

4.1.4.35.

*N'-((3,4-Dichlorobenzyl)sulfonyl)-N-(3-fluoro-4-((6-methoxy-7-(3-(piperidin-1-yl)propoxy)quinolin-4-yl)oxy)phenyl)-3-methoxypropanamidine (**26ai**)*

Yellow solid, yield: 67%, m.p.: 113–115 °C. ^{1}H NMR (400 MHz, $CDCl_3$) δ 9.06 (s, 1 H), 8.50 (d, *J* = 4.8 Hz, 1 H), 7.56 (dd, *J* = 2.0, 8.8 Hz, 1 H), 7.54 (s, 1 H), 7.51 (d,*J* = 1.6 Hz, 1 H), 7.41 (s, 1 H), 7.35–7.33 (m, 1 H), 7.28–7.27 (m, 1 H), 7.21 (t, *J* = 8.4 Hz, 1 H), 7.13–7.11 (m, 1 H), 6.39 (d, *J* = 4.8 Hz, 1 H), 4.26 (s, 2 H), 4.19 (t, *J* = 5.2 Hz, 2 H), 4.00 (s, 3 H), 3.74 (t, *J* = 5.2 Hz, 2 H), 3.43 (s, 3 H), 3.25 (t, *J* = 5.2 Hz, 2 H), 3.07–3.03 (m, 2 H), 2.94–2.86 (m, 4 H), 2.29–2.23 (m, 2 H), 1.81–1.75 (m, 2 H), 1.57–1.50 (m, 4 H). ^{13}C NMR (100 MHz, $CDCl_3$) δ 165.6, 159.9, 154.1 (d, *J* = 248.7 Hz), 151.8, 149.8, 148.9, 146.7, 138.4 (d, *J* = 12.1 Hz), 135.6 (d, *J* = 9.4 Hz), 132.9, 132.7, 132.6, 130.5, 130.3, 130.1, 123.6, 118.5, 115.9, 111.8 (d, *J* = 22.5 Hz), 109.1, 102.5, 99.7, 68.9, 66.3, 59.8, 59.0, 56.1, 55.3, 53.8, 34.1, 24.2, 23.3, 22.5. Anal. Calcd. For $C_{35}H_{39}Cl_2FN_4O_6S$: C, 57.30; H, 5.36; N, 7.64. Found: C, 57.31; H, 5.36; N, 7.66. ESI-MS: *m*/*z* 733.2 $[M+H]^+$.

4.1.4.36.

*N'-((4-Chlorobenzyl)sulfonyl)-N-(3-fluoro-4-((6-methoxy-7-(3-(4-methylpiperazin-1-yl)propoxy)quinolin-4-yl)oxy)phenyl)-3-methoxypropanamidine (**26aj**)*

Yellow solid, yield: 56%, m.p.: 132–134 °C. ^{1}H NMR (400 MHz, $CDCl_3$) δ 8.90 (br s, 1 H), 8.50 (d, *J* = 5.2 Hz, 1 H), 7.62 (dd, *J* = 2.0, 12.0 Hz, 1 H), .7.56 (s, 1 H), 7.43 (s, 1 H), 7.37 (d, *J* = 8.4 Hz, 2 H), 7.31 (d, *J* = 8.0 Hz, 2 H), 7.19 (t, *J* = 8.4 Hz, 1 H), 7.02–7.00 (m, 1 H), 6.37 (d, *J* = 5.2 Hz, 1 H), 4.30 (s, 2 H), 4.25 (t, *J* = 6.8 Hz, 2 H), 4.04 (s, 3 H), 3.72 (t, *J* = 5.2 Hz, 2 H), 3.45 (s, 3 H), 3.24 (t, *J* = 5.2 Hz, 2 H), 2.59 (t, *J* = 7.2 Hz, 4 H), 2.53–2.48 (m, 6 H), 2.31 (s, 3 H), 2.16-2.09 (m, 2 H). ^{13}C NMR (100 MHz, $CDCl_3$) δ 165.5, 159.9, 154.2 (d, *J* = 248.3 Hz), 152.5, 150.1, 148.8, 147.1, 138.4 (d, *J* = 12.2 Hz), 135.6 (d, *J* = 9.4 Hz), 134.7, 132.2, 128.9, 128.4, 123.6, 118.2 (d, *J* = 3.2 Hz), 115.5, 111.9 (d, *J* = 22.8 Hz), 108.9, 102.2, 99.5, 68.8, 67.4, 60.3, 59.0, 56.3, 55.1, 54.9, 53.0, 45.9, 33.9, 26.4. Anal. Calcd. For $C_{35}H_{41}ClFN_5O_6S$: C, 58.86; H, 5.79; N, 9.81. Found: C, 58.88; H, 5.77; N, 9.84. ESI-MS: *m*/*z* 714.3 $[M+H]^+$.

4.1.4.37.

*N'-((3,4-Dichlorobenzyl)sulfonyl)-N-(3-fluoro-4-((6-methoxy-7-(3-(4-methylpiperazin-1-yl)propoxy)quinolin-4-yl)oxy)phenyl)-3-methoxypropanamidine (**26ak**)*

Yellow solid, yield: 53%, m.p.: 118–120 °C. ^{1}H NMR (400 MHz, $CDCl_3$) δ 9.02 (br s, 1 H), 8.48 (d, *J* = 4.0 Hz, 1 H), 7.55 (s, 1 H), 7.51 (dd, *J* = 2.0, 11.6 Hz, 2 H), 7.42 (s, 1 H), 7.39 (d, *J* = 8.0 Hz, 1 H), 7.26 (dd, *J* = 1.6, 8.4 Hz, 1 H), 7.21 (t, *J* = 8.4 Hz, 1 H), 7.10–7.08 (m, 1 H), 6.38 (d, *J* = 4.8 Hz, 1 H), 4.26 (s, 2 H), 4.23–4.22 (m, 2 H), 4.02 (s, 3 H), 3.73 (t, *J* = 5.2 Hz, 2 H), 3.43

(s, 3 H), 3.23 (t, *J* = 5.2 Hz, 2 H), 2.62–2.58 (m, 10 H), 2.36 (s, 3 H), 2.14–2.08 (m, 2 H). ^{13}C NMR (100 MHz, $CDCl_3$) δ 165.6, 159.8, 154.1 (d, *J* = 249.1 Hz), 152.4, 150.0, 148.7, 146.9, 138.5 (d, *J* = 12.4 Hz), 135.4 (d, *J* = 9.0 Hz), 132.9, 132.7, 132.6, 130.5, 130.2, 130.1, 123.6, 118.5 (d, *J* = 3.0 Hz), 115.5, 111.8 (d, *J* = 22.6 Hz), 108.7, 102.3, 99.5, 68.8, 67.2, 59.7, 59.0, 56.2, 54.8, 54.7, 52.4, 45.4, 34.0, 26.2. Anal. Calcd. For $C_{35}H_{40}Cl_2FN_5O_6S$: C, 56.15; H, 5.39; N, 9.35. Found: C, 56.14; H, 5.41; N, 9.36. ESI-MS: *m*/*z* 748.2 $[M+H]^+$.

4.1.4.38.

N'-((4-Chlorobenzyl)sulfonyl)-N-(3-fluoro-4-((6-methoxy-7-(3-(4-methylpiperidin-1-yl)propoxy)quinolin-4-yl)oxy)phenyl)-3-methoxypropanamidine ***(26al)***

Yellow solid, yield: 59%, m.p.: 110–113 °C. ^{1}H NMR (400 MHz, $CDCl_3$) δ 9.24 (br s, 1 H), 8.47 (d, *J* = 5.2 Hz, 1 H), 7.64 (dd, *J* = 2.0, 12.0 Hz, 1 H), 7.53 (s, 1 H), 7.37 (s, 1 H), 7.34 (d, *J* = 8.4 Hz, 2 H), 7.27 (d, *J* = 8.4 Hz, 2 H), 7.17–7.09 (m, 2 H), 6.35 (d, *J* = 4.8 Hz, 1 H), 4.27 (s, 2 H), 4.21 (t, *J* = 5.6 Hz, 2 H), 3.98 (s, 3 H), 3.71 (t, *J* = 5.2 Hz, 2 H), 3.38 (s, 3 H), 3.28–3.25 (m, 2 H), 3.21 (t, *J* = 5.6 Hz, 2 H), 2.95 (t, *J* = 7.2 Hz, 2 H), 2.46–2.40 (m, 2 H), 2.34–2.30 (m, 2 H), 1.73–1.70 (m, 2 H), 1.62–1.53 (m, 3 H), 0.94 (d, *J* = 6.0 Hz, 3 H). ^{13}C NMR (100 MHz, $CDCl_3$) δ 165.4, 159.9, 154.0 (d, *J* = 248.1 Hz), 151.9, 149.7, 148.7, 146.7, 138.0 (d, *J* = 12.6 Hz), 135.8 (d, *J* = 9.4 Hz), 134.5, 132.1, 128.7, 128.4, 123.4, 118.3, 115.6, 111.7 (d, *J* = 22.7 Hz), 108.9, 102.3, 99.6, 69.0, 66.6, 60.2, 58.9, 56.1, 55.0, 53.3, 34.2, 31.9, 29.6, 24.8, 21.1. Anal. Calcd. For $C_{36}H_{42}ClFN_4O_6S$: C, 60.62; H, 5.94; N, 7.86. Found: C, 60.65; H, 5.95; N, 7.88. ESI-MS: *m*/*z* 713.3 $[M+H]^+$.

4.1.4.39.

N'-((3,4-Dichlorobenzyl)sulfonyl)-N-(3-fluoro-4-((6-methoxy-7-(3-(4-methylpiperidin-1-yl)propoxy)quinolin-4-yl)oxy)phenyl)-3-methoxypropanamidine ***(26am)***

Yellow solid, yield: 56%, m.p.: 107–109 °C. ^{1}H NMR (400 MHz, $CDCl_3$) δ 9.23 (s, 1 H), 8.48 (d, *J* = 4.8 Hz, 1 H), 7.58 (d, *J* = 12.4 Hz, 1 H), 7.54 (s, 1 H), 7.49 (s, 1 H), 7.37 (d, *J* = 8.0 Hz, 2 H), 7.24-7.14 (m, 3 H), 6.38 (d, *J* = 4.8 Hz, 1 H), 4.25 (s, 2 H), 4.22 (t, *J* = 6.0 Hz, 2 H), 3.99 (s, 3 H), 3.73 (t, *J* = 5.2 Hz, 2 H), 3.40 (s, 3 H), 3.33–3.30 (m, 2 H), 3.23 (t, *J* = 5.2 Hz, 2 H), 3.00 (t, *J* = 7.6 Hz, 2 H), 2.49 (t, *J* = 9.2 Hz, 2 H), 2.38–2.34 (m, 2 H), 1.76–1.73 (m, 2 H), 1.67–1.53 (m, 3 H), 0.96 (d, *J* = 6.0 Hz, 3 H). ^{13}C NMR (100 MHz, $CDCl_3$) δ 165.6, 159.8, 154.0 (d, *J* = 248.6 Hz), 151.9, 149.8, 148.8, 146.7, 138.3 (d, *J* = 12.2 Hz), 135.7 (d, *J* = 9.1 Hz), 132.8, 132.6, 130.5, 130.3, 130.2, 123.5, 118.5 (d, *J* = 3.1 Hz), 115.8, 111.8 (d, *J* = 22.7 Hz), 109.0, 102.6, 99.7, 68.9, 66.5, 59.7, 59.0, 56.1, 55.0, 53.3, 34.2, 31.7, 29.6, 24.6, 21.1. Anal. Calcd. For $C_{36}H_{41}Cl_2FN_4O_6S$: C, 57.83; H, 5.53; N, 7.49. Found: C, 57.82; H, 5.56; N, 7.51. ESI-MS: *m*/*z* 769.2 $[M+Na]^+$.

4.2. Biology

4.2.1. Cytotoxicity against tumor cells assay

The cancer cells were cultured in minimum essential medium (MEM) supplemented with 10% fetal bovine serum (FBS). Approximately 4×10^3 cells per well, suspended in MEM medium, were plated onto each well of a 96-well plate and incubated in 5% CO_2 at 37 °C for 24 h. The test compounds were added to the culture medium at the indicated final concentrations and the cell cultures were continued for 72 h. Fresh MTT was added to each well at a final concentration of 5 μg/mL and incubated with cells at 37 °C for 4 h. The formazan crystals were dissolved in 100 μL of DMSO per each well, and the absorbency at 492 nm (for the absorbance of MTT formazan) and 630 nm (for the reference wavelength) was measured with the ELISA reader. All compounds were tested three times in each of the cell lines. The results expressed as IC_{50} (inhibitory concentration of 50%) were the average of three determinations calculated by using the Bacus Laboratories Incorporated Slide Scanner (Bliss) software.

4.2.2. Tyrosine kinases assay

The tyrosine kinases activities were evaluated using homogeneous time-resolved fluorescence (HTRF) assays, as previously reported protocol [71]. Briefly, 20 mg/mL poly (Glu, Tyr) 4:1 (Sigma) was preloaded as a substrate in 384-well plates. Then 50 μL of 10 mM ATP (Invitrogen) solution diluted in kinase reaction buffer (50 mM HEPES, pH 7.0, 1 M DTT, 1 M $MgCl_2$, 1 M $MnCl_2$, and 0.1% NaN_3) was added to each well. Various concentrations of compounds diluted in 10 μL of 1% DMSO (v/v) were used as the negative control. The kinase reaction was initiated by the addition of purified tyrosine kinase proteins diluted in 39 μL of kinase reaction buffer solution. The incubation time for the reactions was at 25 °C for 30 min, and the reactions were stopped by the addition of 5 μL of Streptavidin-XL665 and 5 μL of Tk Antibody Cryptate working solution to all of wells. The plates were read using Envision (PerkinElmer) at 320 nm and 615 nm. The inhibition rate (%) was calculated using the following equation: % inhibition 100 = [(Activity of enzyme with tested compounds - Min)/(Max -Min)] × 100 (Max: the observed enzyme activity measured in the presence of enzyme, substrates, and cofactors; Min: the observed enzyme activity in the presence of substrates, cofactors and in the absence of enzyme). IC_{50} values were calculated from the inhibition curves.

4.2.3. Induction of apoptosis and cell cycle analysis

4.2.3.1. Analysis of cellular apoptosis

Apoptosis was detected by an Annexin V-FITC/propidium iodide double staining kit (BD Biosciences) since AnnexinV-fluorescein isothiocyanate (Annexin V-FITC) is a protein that possesses high affinity to phosphatidyl serine PS, which can be detected by staining with Annexin V-FITC and counter staining with propidium iodide (PI). A549 cells were seeded in 6-well plates and allowed to grow for 24 h in culture medium and then treated with vehicle, 1.0 μM of foretinib, 0.25, 0.5 and 1.0 μM of **26af**. The cells were incubated at 37 °C, 5% CO_2 for 12 h. Cells were harvested by centrifugation at 2000 r/min for 5 min and washed with ice-cold PBS solution. The supernatant was abandoned and 195 μL of Annexin V-FITC binding buffer solution (10 mM HEPES, 140 mM NaCl, and 2.5 mM $CaCl_2$ at pH 7.4) was added to resuspend the cells. Afterwards, 5

μL of Annexin V-FITC and 10 μL of propidium iodide staining solution were added and the solution was mixed gently. Next, these samples were incubated in dark at room temperature for 30 min and the labeled cells were analyzed by flow cytometer (FACScan, Bection Dickinson).

4.2.3.2.Flow cytometric analysis of cellcycle distribution

Cell cycle analysis was carried out through flow cytometer. A549 cells were seeded in 6-well plates (3×10^5 cells/well), incubated in the presence or absence of **26af** and foretinib at the indicated concentrations at 37 °C for 24 h, 5% CO_2. Cells were washed twice with phosphate buffer saline, harvested by centrifugation and then fixed in ice-cold 70% ethanol overnight. After the ethanol was removed the next day, the cells were resuspended in ice-cold PBS, treated with RNase A (Keygen Biotech, China) at 37 °C for 30 min, and then incubated with the DNA staining solution propidium iodide (PI, Keygen Biotech, China) at 4 °C for 30 min. DNA cell cycle profiling was determined by measuring DNA content by using flow cytometer (FACScan, Bection Dickinson), and the percentage of G1, S, G2/M cells was calculated by using ModFit LT version 3.0.

4.2.4. Western Blotting analysis

A549 cells were cultured under regular growth conditions to the exponential growth phase. Then A549 cells (5.0×10^5 cells/dish) were incubated with or without **26af** at various concentrations for 6 h. After incubation, the cells were collected by centrifugation and washed twice with phosphate-buffered saline chilled to 0 °C. The cells were homogenized in RIPA lysis buffer containing 150 mM NaCl, 50 mM Tris (pH 7.4), 1% (w/v) sodium deoxycholate, 1% (v/v) Triton X-100, 0.1% (w/v) SDS, and 1 mM EDTA (Beyotime, China). The lysates were incubated on ice for 30 min, intermittently vortexed every 5 min, and centrifuged at 12 500 g for 15 min to harvest the supernatants. Next, the protein concentrations were determined by a BCA Protein Assay Kit (Thermo Fisher Scientific, Rockford, Illinois, USA). The protein extracts were reconstituted in loading buffer containing 62 mM Tris-HCl, 2% SDS, 10% glycerol, and 5% β-mercaptoethanol (Beyotime, China), and the mixture was boiled at 100 °C for 10 min. An equal amount of the proteins (50 mg) was separated by 8–12% sodium dodecyl sulfate-polyacrylamide gel electrophoresis (SDS-PAGE) and transferred to nitrocellulose membranes (Amersham Biosciences, Little Chalfont, Buckinghamshire, UK). Then, the membranes were blocked with 5% nonfat dried milk in TBS containing 1% Tween-20 for 90 min at room temperature and were incubated overnight with specific primary antibodies (CST, USA) at 4 °C. After washing three times with TBS, the membranes were incubated with the appropriate HRP-conjugated secondary antibodies at room temperature for 2 h. The blots were developed with enhanced chemiluminescence (Pierce, Rockford, Illinois, USA) and were detected by an LAS4000 imager (GE Healthcare, Waukesha, Wisconsin, USA).

4.2.5. Acute toxicity test

Sixty 8-week-old male BALB/c mice (SLRC Laboratory Animal Inc., Shanghai, China) were used to evaluate single-dose toxicity. Mice were randomly divided into six groups (n = 10) and received a single intraperitoneal injection of **26af** at 0 (vehicle), 100, 200, 300, or 400 mg/kg on day 0, respectively. One group was untreated as the normal control. The mouse death was monitored daily, body weight was measured every 3 days for 15 days. At the end of experimental period, all animals were euthanized by CO_2 and necropsied for gross lesion examination for possible damage to the heart, liver, and kidneys. And tissues from the liver, lung, kidney, and spleen were weighed (data not shown).

4.2.6. Pharmacokinetic profiles of the selected compound

The pharmacokinetic parameters of **26af** was determined in BALB/c mice (SLRC Laboratory Animal Inc., Shanghai, China). A total of 12 mice were randomly divided into two groups in this study (n = 6 each for i.v. and p.o. group). The mice were fasted overnight prior to dosing and fed 4 h postdose. Three serum samples were collected from each mouse, the first two samples by retro-orbital bleed and the third sample by cardiac puncture. Each animal received a single **26af** as a solution in PEG 400/water (70:30) by either oral administration (8 mg/kg) or intravenous injection (2 mg/kg). Blood samples were collected into the microcentrifuge tubes containing heparin at 5, 10, 20 min, 0.5, 1, 3, 6, 8, 10, 12, and 24 h time points following iv dosing and at 5, 10, 20 min, 0.5, 1, 3, 6, 8, 10, 12, and 24 h following oral dosing. The blood samples were centrifuged at 8000 rmp for 5 min and the plasmas were stored at -20 °C until analysis. The plasma samples were deproteinized with acetonitrile containing an internal standard. The mixture was vortex-mixed thoroughly for 10 min at 1500 rpm, and then centrifuged at 6000 g for 10 min. The supernatant was transferred to another clean 96 deep-well plate and centrifuged again at 6000 g for 10 min. Finally, the compound concentrations in supernatant were measured by LC/MS/MS. The results were shown as the maximum plasma concentration (C_{max}), the time to reach peak plasma concentration (T_{max}), terminal half-life ($T_{1/2}$), the area under the plasma concentration-time curve from zero to time infinity ($AUC_{0-\infty}$), the total clearance (*CL*) and bioavailability (*F*).

4.3. Docking studies

For docking purposes, the three-dimensional structure of the c-Met (PDB code: 3LQ8) and VEGFR-2 (PDB code: 3U6J) were obtained from RCSB Protein Data Bank [72]. Hydrogen atoms were added to the structure allowing for appropriate ionization at physiological pH. The protonated state of several important residues was adjusted by using SYBYL 6.9.1 (Tripos, St. Louis, USA) in favor of forming reasonable hydrogen bond with the ligand. Molecular docking analysis was carried out by the Autodock 4.2 package to explore the binding model for the active site of c-Met or VEGFR-2 with its corresponding ligand. All atoms located within the range of 5.0 Å from any atom of the cofactor were selected into the active site, and the corresponding amino acid residue was, therefore, involved into the active binding site if only one of its atoms was selected. Other parameters were all set as default in the docking calculations. All calculations were performed on Silicon Graphics workstation. Then, in

order to check the stability of protein-ligand complex, the best docking conformations that with the lowest docking energy (c-Met/**26af**, VEGFR-2/**26af**) and the crystal structureof c-Met/foretinib were employed for molecular dynamics (MD) simulations. It was carried out by AMBER software (version 16), using AMBER ff99sb force field for complex [73]. Hydrogen atoms were added to the initial c-Met/**26af** and VEGFR-2/**26af** complex model using the leap module, setting ionizable residues as their default protonation states at a neutral pH value. The complex was solvated in a cubic periodic box of explicit TIP3P water model that extended a minimum 10 Å distance from the box surface to any atom of the solute. All bond lengths were constrained using the SHAKE algorithm and integration time step was set to 2 fs using the Verlet leapfrog algorithm. To eliminate possible bumps between the solute and the solvent, the entire systems was minimized in two steps. Firstly, the complex was restrained with a harmonic potential of the form $k(\Delta x)^2$ with a force constant k = 100 kcal/mol^{-1}·Å^{-2}. The water molecules and counter ions were optimized using the steepest descent method, followed by the conjugate gradient method. Secondly, the entire system was optimized by using the first step method without any constraint. These two minimization steps were followed by annealing simulation with a weak restraint (k = 100 kcal/mol^{-1}·Å^{-2}) for the complex and the entire system was heated gradually in the NVT ensemble from 0 to 298 K over 500 ps. After the heating phase, a 10 ns MD simulation was performed under 1 atm. The constant temperature was selected at 298 K with the NPT ensemble. Constant temperature was maintained using the Langevin thermostat with a collision frequency of 2 ps^{-1}. The constant pressure was maintained employing isotropic position scaling algorithm with a relaxation time of 2 ps. Based on the final 10 ns MDs trajectory, 3000 snapshots were extracted from the last 3 ns trajectory for the refined binding model.

Declaration of competing interest

The authors declare no competing financial interest or personal relationships that could have appeared to influence the work reported in this paper.

Author Contributions

X. Nan, J. Zhang, R. Wu, S.B. Fang, H.J. Li and Z.Z. Zhang conducted the research, analyzed the data, and wrote the manuscript. H.J. Li, R. Wu, S.B. Fang and Y.C. Wu designed the study, analyzed the data, wrote the manuscript and commented on the manuscript.

Acknowledgements

This work was supported by Key Research and Development Program of Shandong Province (2019GSF108089), Natural Science Foundation of Shandong Province (ZR2019MB009), National Natural Science Foundation of China (21672046, 21372054), and Found from the Huancui District of Weihai City.

Appendix A. Supplementary data

Supplementary data related to this article can be found athttps://doi.org/10.1016/j.xxxxx.xxxx.xx.xxx.

References

[1] D.P. Bottaro, J.S. Rubin, D.L. Faletto, A.M.-L. Chan, T.E. Kmiecik, G.F. Vande Woude, S.A. Aaronson, Identification of the hepatocyte growth factor receptor as the c-*met* proto-oncogene product, Science 251 (1991) 802–804.

[2] M. Dean, M. Park, M.M. Le Beau, T.S. Robins, M.O. Diaz, J.D. Rowley, D.G. Blair, G.F. Vande Woude, The human *met* oncogene is related to the tyrosine kinase oncogenes, Nature 318 (1985) 385–388.

[3] C. Birchmeier, W. Birchmeier, E. Gherardi, G.F. Vande Woude, Met, metastasis, motility and more, Nat. Rev. Mol. Cell Biol. 4 (2003) 915–925.

[4] W. Gao, J.K. Han, Overexpression of ING5 inhibits HGF-induced proliferation, invasion and EMT in thyroid cancer cells via regulation of the c-Met/PI3K/Akt signaling pathway, Biomed. Pharmacother. 98 (2018) 265–270.

[5] J.A. Aguirre Ghiso, D.F. Alonso, E.F. Farías, D.E. Gomez, E.B. de Kier Joffè, Deregulation of the signaling pathways controlling urokinase production, Eur. J. Biochem. 263 (1999) 295–304.

[6] P.K. Parikh, M.D. Ghate, Recent advances in the discovery of small molecule c-Met Kinase inhibitors, Eur. J. Med. Chem. 143 (2018) 1103–1138.

[7] J.J. Hu, X. Li, J.X. Zhou, C. Zhang, G.H. Zheng, Z.P. Qiu, Celastrol delays hepatic steatosis and carcinogenesis in a rapid AKT/c-Met-transfected hepatocellular carcinoma model *via* suppressing fatty acid synthase expression and AKT/ERK phosphorylation, RSC Adv. 8 (2018) 13976–13983.

[8] M. Jeffers, S. Rong, M. Anver, G.F. Vande Woude, Autocrine hepatocyte growth factor/scatter factor-Met signaling induces transformation and the invasive/metastastic phenotype in C127 cells, Oncogene 13 (1996) 853–856.

[9] H. Takayama, W.J. LaRochelle, R. Sharp, T. Otsuka, P. Kriebel, M. Anver, S.A. Aaronson, G. Merlino, Diverse tumorigenesis associated with aberrant development in mice overexpressing hepatocyte growth factor/scatter factor, P. Natl. Acad. Sci. USA 94 (1997) 701–706.

[10] T. Otsuka, H. Takayama, R. Sharp, G. Celli, W.J. LaRochelle, D.P. Bottaro, N. Ellmore, W. Vieira, J.W. Owens, M. Anver, G. Merlino, c-Met autocrine activation induces development of malignant melanoma and acquisition of the metastatic phenotype, Cancer Res. 58 (1998) 5157–5167.

[11] S. Baldacci, Z. Kherrouche, V. Cockenpot, L. Stoven, M.C. Copin, E. Werkmeister, N. Marchand, M. Kyheng, D. Tulasne, A.B. Cortot, MET amplification increases the metastatic spread of EGFR-mutated NSCLC, Lung Cancer 125 (2018) 57–67.

[12] G. Tsakonas, J. Botling, P. Micke, C. Rivard, L. LaFleur, J. Mattsson, T. Boyle, F.R. Hirsch, S. Ekman, c-MET as a biomarker in patients with surgically resected non-small cell lung cancer, Lung Cancer 133 (2019) 69–74.

[13] Y. Toiyama, C. Miki, Y. Inoue, Y. Okugawa, K. Tanaka, M. Kusunoki, Serum hepatocyte growth factor as a prognostic marker for stage II or III colorectal cancer patients, Int. J. Cancer 125 (2009) 1657–1662.

[14] J.G. Christensen, J. Burrows, R. Salgia, c-Met as a target for human cancer and characterization of inhibitors for therapeutic intervention, Cancer Lett. 225 (2005) 1–26.

[15] L. Tao, J.X. Qiu, S. Slavin, Z.Y. Ou, Z.H. Liu, J.F. Ge, L. Zuo, E.A. Guancial, E.M. Messing, C. Chang, S. Yeh, Recruited T cells promote the bladder cancer metastasis *via* upregulation of the estrogen receptor β/IL-1/c-MET signals, Cancer Lett. 430 (2018) 215–223.

[16] F. Cappuzzo, A. Marchetti, M. Skokan, E. Rossi, S. Gajapathy, L. Felicioni, M. del Grammstro, M.G. Sciarrotta, F. Buttitta, M. Incarbone, L. Toschi, G. Finocchiaro, A. Destro, L. Terracciano, M. Roncalli, M. Alloisio, A. Santoro, M. Varella-Garcia, Increased MET gene copy number negatively affects survival of surgically resected non-small-cell lung cancer patients, J. Clin. Oncol. 27 (2009) 1667–1674.

[17] N. Li, Z.F. Dou, J.C. Liu, B. Chai, Y. Li, X.Q. An, P.L. Chu, X.L. Zhang, Therapeutic effect of HGF on NASH mice through HGF/c-Met and JAK2-STAT3 signalling pathway, Ann. Hepatol. 17 (2018) 501–510.

[18] B. Cao, Y. Su, M. Oskarsson, P. Zhao, E.J. Kort, R.J. Fisher, L.M. Wang, G.F. Vande Woude, Neutralizing monoclonal antibodies to hepatocyte growth factor/scatter factor (HGF/SF) display antitumor activity in animal models, P. Natl. Acad. Sci. USA 98 (2001) 7443–7448.

[19] K.J. Kim, L. Wang, Y.C. Su, G.Y. Gillespie, A. Salhotra, B. Lal, J. Laterra, Systemic anti-hepatocyte growth factor monoclonal antibody therapy induces the regression of intracranial glioma xenografts, Clin. Cancer Res. 12 (2006) 1292–1298.

[20] D. Tomioka, N. Maehara, K. Kuba, K. Mizumoto, M. Tanaka, K. Matsumoto, T. Nakamura, Inhibition of growth, invasion, and metastasis of human pancreatic carcinoma cells by NK4 in an orthotopic mouse model, Cancer Res. 61 (2001) 7518–7524.

[21] M.A. Brockmann, A. Papadimitriou, M. Brandt, R. Fillbrandt, M. Westphal, K. Lamszus, Inhibition of intracerebral glioblastoma growth by local treatment with the scatter factor/hepatocyte growth factor-antagonist NK4, Clin. Cancer Res. 9 (2003) 4578–4585.

[22] P. Michieli, M. Mazzone, C. Basilico, S. Cavassa, A. Sottile, L. Naldini, P.M. Comoglio, Targeting the tumor and its microenvironment by a dual-function decoy Met receptor, Cancer Cell 6 (2004) 61–73.

[23] R. Abounader, S. Ranganathan, B. Lal, K. Fielding, A. Book, H. Dietz, P. Burger, J. Laterra, Reversion of human glioblastoma malignancy by U1 small nuclear RNA/ribozyme targeting of scatter factor/hepatocyte growth gactor and c-Met expression, J. Natl. Cancer Inst. 91 (1999) 1548–1556.

[24] S.J. Hachey, C.C.W. Hughes, Applications of tumor chip technology, Lab Chip 18 (2018) 2893–2912.

[25] F. Shi, Y.B. Zhang, J. Wang, J. Su, Z. Liu, T. Wang, RNA-sequencing identified miR-3681 as a negative regulator in the proliferation and migration of cervical cancer cells *via* the posttranscriptional suppression of HGFR, RSC Adv. 9 (2019) 22376–22383.

[26] H.K. Jin, R.H. Yang, Z. Zheng, M. Romero, J. Ross, H. Bou-Reslan, R.A.D. Carano, I. Kasman, E. Mai, J. Young, J.P. Zha, Z.M. Zhang, S. Ross, R. Schwall, G. Colbern, M. Merchant, MetMAb, the one-armed 5D5 anti-c-Met antibody, inhibits orthotopic pancreatic tumor growth and improves survival, Cancer Res. 68 (2008) 4360–4368.

[27] I. Dussault, S.F. Bellon, From concept to reality: the long road to c-Met and RON receptor tyrosine kinase inhibitors for the treatment of cancer, Anti-cancer Agents Med. Chem. 9 (2009) 221–229.

[28] W.H. Wang, S. Xu, Y.L. Du, X.B. Liu, X.J. Li, C.L. Wang, B.B. Zhao, P.W. Zheng, W.F. Zhu, Synthesis and bioevaluation and doking study of 1*H*-pyrrolo[2,3-b]pyridine derivatives bearing aromatic hydrazone moiety as c-Met inhibitors, Eur. J. Med. Chem. 145 (2018) 315–327.

[29] L.S. Zhuo, H.C. Xu, M.S. Wang, X.E. Zhao, Z.H. Ming, X.L. Zhu, W. Huang, G.F. Yang, 2,7-Naphthyridinone-based MET kinase inhibitors: a promising novel scaffold for antitumor drug development, Eur. J. Med. Chem. 178 (2019) 705–714.

[30] J. Liu, Y.L. Gong, J.T. Shi, X.C. Hao, Y. Wang, Y.P. Zhou, Y.L. Hou, Y.J. Liu, S. Ding, Y. Chen, Design, synthesis and biological evaluation of novel *N*-[4-(2-fluorophenoxy)pyridin-2-yl]cyclopropanecarboxamide derivatives as potential c-Met kinase inhibitors, Eur. J. Med. Chem. 194 (2020) 112244.

[31] W.M. Rashed, c-Met as a potential target therapy toward personalized therapy in some pediatric tumors: an overview, Crit. Rev. Oncol. Hemat. 131 (2018) 7–15.

[32] X. Zhai, G.L. Bao, L.M. Wang, M.K. Cheng, M. Zhao, S.J. Zhao, H.Y. Zhou, P. Gong, Design, synthesis and biological evaluation of novel 4-phenoxy-6,7-disubstituted quinolines possessing (thio)semicarbazones as c-Met kinase inhibitors, Bioorg. Med. Chem. 24 (2016) 1331–1345.

[33] H.L. Yuan, Q.F. Liu, L. Zhang, S.H. Hu, T.T. Chen, H.F. Li, Y.D. Chen, Y.C. Xu, T. Lu, Discovery, optimization and biological evaluation for novel c-Met kinase inhibitors, Eur. J. Med. Chem. 143 (2018) 491–502.

[34] X. Nan, H.J. Li, S.B. Fang, Q.Y. Li, Y.C. Wu, Structure-based discovery of novel 4-(2-fluorophenoxy)quinoline derivatives as c-Met inhibitors using isocyanide-involved multicomponent reactions, Eur. J. Med. Chem. 193 (2020) 112241.

[35] S. Matsumoto, N. Miyamoto, T. Hirayama, H. Oki, K. Okada, M. Tawada, H. Iwata, K. Nakamura, S. Yamasaki, H. Miki, A. Hori, S. Imamura, Structure-based design, synthesis, and evaluation of imidazo[1,2-b]pyridazine and imidazo[1,2-a]pyridine derivatives as novel dual c-Met and VEGFR2 kinase inhibitors, Bioorg. Med. Chem. 21 (2013) 7686–7698.

[36] J.J. Cui, M. Tran-Dubé, H. Shen, M. Nambu, P.P. Kung, M. Pairish, L. Jia, J. Meng, L. Funk, I. Botrous, M. McTigue, N. Grodsky, K. Ryan, E. Padrique, G. Alton, S. Timofeevski, S. Yamazaki, Q.H. Li, H. Zou, J. Christensen, B. Mroczkowski, S. Bender, R.S. Kania, M.P. Edwards, Structure based drug design of crizotinib (PF-02341066), a potent and selective dual inhibitor of mesenchymal-epithelial transition factor (c-MET) kinase and anaplastic lymphoma kinase (ALK), J. Med. Chem. 54 (2011) 6342–6363.

[37] M.M. Liu, Y.L. Hou, W.L. Yin, S.G. Zhou, P. Qian, Z. Guo, L.Y. Xu, Y.F. Zhao, Discovery of a novel 6,7-disubstituted-4-(2-fluorophenoxy)quinolines bearing 1,2,3-triazole-4-carboxamide moiety as potent c-Met kinase inhibitors, Eur. J. Med. Chem. 119 (2016) 96–108.

[38] B.H. Qi, Y. Yang, G.W. Gong, H. He, X.P. Yue, X. Xu, Y. Hu, J.M. Li, T. Chen, X.B. Wan, A.M. Zhang, G.B. Zhou, Discovery of N^1-(4-((7-(3-(4-ethylpiperazin-1-yl)propoxy)-6-methoxyquinolin-4-yl)oxy)-3,5-difluorophenyl)-N^3-(2-(2,6-difluorophenyl)-4-oxothiazolidin-3-yl) urea as a multi-tyrosine kinase inhibitor for drug-sensitive and drug-resistant cancers treatment, Eur. J. Med. Chem. 163 (2019) 10–27.

[39] E.J. Wiest, H. Jensen Smith, M. A. Hollingsworth, Met receptor inhibitor SU11274 localizes in the endoplasmic reticulum, Biochem. Biophys. Res. Commun. 501 (2018) 858–862.

[40] T.L. Underiner, T. Herbertz, S.J. Miknyoczki, Discovery of small molecule c-Met inhibitors: evolution and profiles of clinical candidates, Anti-Cancer Agents Med. Chem. 10 (2010) 7–27.

[41] J. Liu, M.H. Nie, Y.J. Wang, J.X. Hu, F. Zhang, Y.L. Gao, Y.J. Liu, P. Gong, Design, synthesis and structure-activity relationships of novel 4-phenoxyquinoline derivatives containing 1,2,4-triazolone moiety as c-Met kinase inhibitors, Eur. J. Med. Chem. 123 (2016) 431–446.

[42] N.D. D'Angelo, S.F. Bellon, S.K. Booker, Y. Chen, A. Coxon, C. Dominguez, I. Fellows, D. Hoffman, R. Hungate, P. Kaplan-Lefko, M.R. Lee, C. Li, L.B. Liu, E. Rainbeau, P.J. Reider, K. Rex, A. Siegmund, Y.X. Sun, A.S. Tasker, N. Xi, S.M. Xu, Y.J. Yang, Y.H. Zhang, T.L. Burgess, I. Dussault, T.S. Kim, Design, synthesis, and biological evaluation of potent c-Met inhibitors, J. Med. Chem. 51 (2008) 5766–5779.

[43] S.J. Zhao, Y. Zhang, H.Y. Zhou, S.C. Xi, B. Zou, G.L. Bao, L.M. Wang, J. Wang, T.F. Zeng, P. Gong, X. Zhai, Synthesis and biological evaluation of 4-(2-fluorophenoxy)-3,3′-bipyridine derivatives as potential c-met inhibitors, Eur. J. Med. Chem. 120 (2016) 37–50.

[44] L.B. Liu, M.H. Norman, M. Lee, N. Xi, A. Siegmund, A.A. Boezio, S. Booker, D. Choquette, N.D. D'Angelo, J. Germain, K. Yang, Y.J. Yang, Y.H. Zhang, S.F. Bellon, D.A. Whittington, J.C. Harmange, C. Dominguez, T.S. Kim, I. Dussault, Structure-based design of novel class II c-Met inhibitors: 2. SAR and kinase selectivity profiles of the pyrazolone series, J. Med. Chem. 55 (2012) 1868–1897.

[45] M. Younas, C. Hano, N. Giglioli-Guivarc'h, B.H. Abbasi, Mechanistic evaluation of phytochemicals in breast cancer remedy: current understanding and future perspectives, RSC Adv. 8 (2018) 29714–29744.

[46] M.E. Shakera, A.A. Shaabanb, M.M. El-Shafeyd, M.E. El-Mesery, The selective c-Met inhibitor capmatinib offsets cisplatin-nephrotoxicity and doxorubicin-cardiotoxicity and improves their anticancer efficacies, Toxicol. Appl. Pharmacol. 398 (2020) 115018.

[47] Q.D. Tang, Y.L. Duan, H.H. Xiong, T. Chen, Z. Xiao, L.X. Wang, Y.Y. Xiao, S.M. Huang, Y.H. Xiong, W.F. Zhu, P. Gong, P.W. Zheng, Synthesis and antiproliferative activity of 6,7-disubstituted-4-phenoxyquinoline derivatives bearing the 1,8-naphthyridin-2-one moiety, Eur. J. Med. Chem. 158 (2018) 201–213.

[48] W.K. Liao, G. Hu, Z. Guo, D.Y. Sun, L.X. Zhang, Y.X. Bu, Y.X. Li, Y.J. Liu, P. Gong, Design and biological evaluation of novel 4-(2-fluorophenoxy)quinoline derivatives bearing an imidazolone moiety as c-Met kinase inhibitors, Bioorg. Med. Chem. 23 (2015) 4410–4422.

[49] W.R.J.D. Galloway, A. Isidro-Llobet, D.R. Spring, Diversity-oriented synthesis as a tool for the discovery of novel biologically active small molecules, Nat. Commun. 1 (2010) 1–13.

[50] D.S. Wei, H.R. Fan, K. Zheng, X.M. Qin, L.F. Yang, Y.J. Yang, Y. Duan, Q. Zhang, C.C. Zeng, L.M. Hu, Synthesis and anti-tumor activity of [1,4]dioxino [2,3-f]quinazoline derivatives as dual inhibitors of c-Met and VEGFR-2, Bioorg. Chem. 88 (2019) 102916.

[51] T.E. Nielsen, S.L. Schreiber, Towards the optimal screening collection: a synthesis strategy, Angew. Chem. Int. Ed. 47 (2008) 48–56.

[52] C. Cordier, D. Morton, S. Murrison, A. Nelson, C. O'Leary-Steele, Natural products as an inspiration in the diversity-oriented synthesis of bioactive compound libraries, Nat. Prod. Rep. 25 (2008) 719–737.

[53] J.V. Greenhill, P. Lue, Amidines and guanidines in medicinal chemistry, Prog. Med. Chem. 30 (1993) 203–326.

[54] T.R.M. Rauws, B.U.W. Maes, Transition metal-catalyzed *N*-arylations of amidines and guanidines, Chem. Soc. Rev. 41 (2012) 2463–2497.

[55] S.M. Sondhi, M. Dinodia, S. Jain, A. Kumar, Synthesis of biologically active *N*-methyl derivatives of amidines and cyclized five-membered products of amidines with oxalyl chloride, Eur. J. Med. Chem. 43 (2008) 2824–2830.

[56] A. Casini, A. Scozzafava, A. Mastrolorenzo, C. T. Supuran, Sulfonamides and sulfonylated derivatives as anticancer agents, Curr. Cancer Drug Tar. 2 (2002) 55–75.

[57] R. Nishino, K. Ikeda, T. Hayakawa, T. Takahashi, T. Suzuki, M. Sato, Syntheses of 2-deoxy-2,3-didehydro-*N*-acetylneuraminic acid analogues modified by *N*-sulfonylamidino groups at the C-4 position and biological evaluation as inhibitors of human parainfluenza virus type 1, Bioorg. Med. Chem. 19 (2011) 2418–2427.

[58] S.H. Cho, S. Chang, Room temperature copper-catalyzed 2-functionalization of pyrrole rings by a three-component coupling reaction, Angew. Chem. Int. Ed. 47 (2008) 2836–2839.

[59] W.J. Yao, L.J. Pan, Y.P. Zhang, G. Wang, X.Q. Wang, C. Ma, Three-component assembly and divergent ring-expansion cascades of functionalized 2-iminooxetanes, Angew. Chem. Int. Ed. 49 (2010) 9210–9214.

[60] I. Bae, H. Han, S. Chang, Highly efficient one-pot synthesis of *N*-sulfonylamidines by Cu-catalyzed three-component coupling of sulfonyl azide, alkyne, and amine, J. Am. Chem. Soc. 127 (2005) 2038–2039.

[61] M.J. Wang, Y.Q. Liu, L.C. Chang, C.Y. Wang, Y.L. Zhao, X.B. Zhao, K.D. Qian, X. Nan, Y. Liu, X.M. Wang, H.Y. Hung, J.S. Yang, D.H. Kuo, M. Goto, S.L. Morris-Natschke, S.L. Pan, C.M. Teng, S.C. Kuo, T.S. Wu, Y.C. Wu, K.H. Lee, Design, synthesis, mechanisms of action, and toxicity of novel 20(*S*)-sulfonylamidine derivatives of camptothecin as potent antitumor agents, J. Med. Chem. 57 (2014) 6008–6018.

[62] A. Flood, C. Trujillo, G. Sanchez-Sanz, B. Kelly, C. Muguruza, L.F. Callado, I. Rozas, Thiophene/thiazole-benzene replacement on guanidine derivatives targeting α_2-adrenoceptors, Eur. J. Med. Chem. 138 (2017) 38–50.

[63] A.P. Gaywood, L. Hill, S.H. Imam, H. McNab, G. Neumajer, W.J. O'Neill, P. Mátyus, Cyclisation reactions of some pyridazinylimidoylketenes, New J. Chem. 34 (2010) 236–242.

[64] M.J. Munchhof, J.S. Beebe, J.M. Casavant, B.A. Cooper, J.L. Doty, R.C. Higdon, S.M. Hillerman, C.I. Soderstrom, E.A. Knauth, M.A. Marx, A.M.K. Rossi, S.B. Sobolov, J.M. Sun, Design and SAR of thienopyrimidine and thienopyridine inhibitors of VEGFR-2 kinase activity, Bioorg. Med. Chem. Lett. 14 (2004) 21–24.

[65] L. Tan, Z. Zhang, D.L. Gao, S.P. Chan, J.F. Luo, Z.C. Tu, Z.M. Zhang, K. Ding, X.M. Ren, X.Y. Lu, Quinolone antibiotic derivatives as new selective Axl kinase inhibitors, Eur. J. Med. Chem. 166 (2019) 318–327.

[66] Y.T. Sun, G.F. Wang, Y.Q. Yang, F.J. Jin, Y.F. Wang, X.Y. Xie, R.H. Mach, Y.S. Huang, Synthesis and pharmacological evaluation of 6,7-dimethoxy-1,2,3,4-tetrahydroisoquinoline derivatives as sigma-2 receptor ligands, Eur. J. Med. Chem. 147 (2018) 227–237.

[67] Z.H. Yang, J.X. Xu, Convenient and environment-friendly synthesis of sulfonyl chlorides from *S*-alkylisothiourea salts via *N*-chlorosuccinimide chlorosulfonation, Synthesis 45 (2013) 1675–1682.

[68] Z.L. Song, M.J. Wang, L.L. Li, D. Wu, Y.H. Wang, L.T. Yan, S.L. Morris-Natschke, Y.Q. Liu, Y.L. Zhao, C.Y. Wang, H.X. Liu, M. Goto, H. Liu, G.X. Zhu, K.H. Lee, Design, synthesis, cytotoxic activity and molecular docking studies of new 20(*S*)-sulfonylamidine camptothecin derivatives, Eur. J. Med. Chem. 115 (2016) 109–120.

[69] M.J. Wang, X.B. Zhao, D. Wu, Y.Q. Liu, Y. Zhang, X. Nan, H.X. Liu, H.T. Yu, G.F. Hu, L.T. Yan, Design, synthesis, crystal structure, insecticidal activity, molecular docking, and QSAR studies of novel N_3-substituted imidacloprid derivatives, J. Agric. Food Chem. 62 (2014) 5429–5442.

[70] X. Nan, Y.F. Jiang, H.J. Li, J.H. Wang, Y.C. Wu, Design, synthesis and evaluation of sulfonylurea-containing 4-phenoxyquinolines as highly selective c-Met kinase inhibitors, Bioorg. Med. Chem. 27 (2019) 2801–2812.

[71] M.L. Peach, N. Tan, S.J. Choyke, A. Giubellino, G. Athauda, T.R. Burke, M.C. Nicklaus, D.P. Bottaro, Directed discovery of agents targeting the Met tyrosine kinase domain by virtual screening, J. Med. Chem. 52 (2009) 943–951.

[72] K.S. Kim, L.P. Zhang, R. Schmidt, Z.W. Cai, D. Wei, D.K. Williams, L.J. Lombardo, G.L. Trainor, D. Xie, Y.Q. Zhang, Y. An, J.S. Sack, J.S. Tokarski, C. Darienzo, A. Kamath, P. Marathe, Y.P. Zhang, J. Lippy, R. Jeyaseelan, B. Wautlet, B. Henley, J. Gullo-Brown, V. Manne, J.T. Hunt, J. Fargnoli, R.M. Borzilleri, Discovery of pyrrolopyridine-pyridone based inhibitors of Met kinase: synthesis, X-ray crystallographic analysis, and biological activities, J. Med. Chem. 51 (2008) 5330–5341.

[73] D.A. Case, T.E. Cheatham III, T. Darden, H. Gohlke, R. Luo, K.M. Merz Jr, A. Onufriev, C. Simmerling, B. Wang, R.J. Woods, The amber biomolecular simulation programs, J. Comput. Chem. 26 (2005) 1668–1688.

Highlights

- 39 novel *N*-sulfonylamidines were designed and synthesized for biological evaluation
- Compound **26af** displayed an IC_{50} value of 2.89 nM against c-Met kinase
- **26af** inhibited A549 cells by inducing apoptosis and G2/M phase cell cycle arrest
- **26af** had desirable pharmacokinetic properties and an acceptable safety profile
- Docking studies indicated the mode of interaction with the binding site of c-Met

The authors declare no competing financial interest or personal relationships that could have appeared to influence the work reported in this paper.